

Article

The Vindolanda Vessel: pXRF and Microphotography of an Enamel-Painted Roman Gladiator Glass

Louisa Campbell

Archaeology, School of Humanities, College of Arts, University of Glasgow, Molema Building, Lilybank Gardens, Glasgow G12 8QQ, UK; louisa.campbell@glasgow.ac.uk

Abstract: Roman glass is well studied and known to have been produced from a mineral soda source and calcareous sand with variation between elements relating to naturally occurring minerals in the sands. While the common characteristics of colourants and opacifiers used in opaque and translucent glasses are well understood, the diverse elemental composition of colouring agents associated with the highly specialised, and largely unexplored, technique of enamel-painted glass has never been firmly established. There remains a significant gap in knowledge of pigments used for this technological innovation which is here addressed through the deployment of non-invasive portable X-Ray Fluorescence (pXRF) analysis and microphotography on a unique Roman enamel-painted gladiator glass from Vindolanda fort. This vanguard research has successfully established, for the first time, a palette of pigments associated with this specialist technique. It is now possible to unravel previously unknown information on complex manufacturing processes and significantly expand the repertoire of the pigments bound up in enamelling recipes used to depict the striking iconographic scenes on the Vindolanda vessel and, potentially, other Roman enamelled glassware. The detection of Cinnabar, Egyptian blue, Orpiment and other pigments are ground-breaking discoveries that will have a transformative impact on early glassmaking studies and push the boundaries of scholarship into new directions of analytical approaches in heritage materials science to complement recent success in this field with Raman spectroscopy and other techniques. The methodology is unprecedented and has been validated through the high quality of the resulting data which permits the extrapolation of elemental compositions of enamelling materials from those associated with the base vessel. This unique approach provides remarkable insights that will revolutionise our understanding of enamelling technologies using the Vindolanda vessel as the investigative platform for forgotten practice.

Keywords: Roman glass; pigments; enamel-painted glass; gladiatorial vessels; pXRF; Vindolanda

Citation: Campbell, L. The Vindolanda Vessel: pXRF and Microphotography of an Enamel-Painted Roman Gladiator Glass. *Heritage* **2023**, *6*, 3638–3672. <https://doi.org/10.3390/heritage6040194>

Academic Editor: Vittoria Guglielmi

Received: 9 March 2023

Revised: 31 March 2023

Accepted: 2 April 2023

Published: 12 April 2023



Copyright: © 2023 by the authors. Submitted for possible open access publication under the terms and conditions of the Creative Commons Attribution (CC BY) license (<https://creativecommons.org/licenses/by/4.0/>).

1. Introduction

The technological aspects of Roman glassmaking traditions are relatively well understood, but specialist techniques and materials associated with enamel-painted glassware are much less so since they have never been comprehensively studied. These rare vessels depict various Roman traditions through vibrantly coloured imagery including mythology; deities; historical events; flora; fauna; and gladiatorial combat. Some colourants common to the enamelling process are known, but the potential presence of pigments articulating this iconography has never been fully established.

This research identifies pigments used in Roman enamel-painting techniques by testing the applicability of *in situ* non-destructive analytical techniques, including portable X-Ray Fluorescence (pXRF) and microphotography. These were deployed, for the first time, on fragile fragments of an exquisite enamel-painted vessel from Vindolanda fort to ascertain elemental composition of surface treatments and investigate how these materials perform at a level not visible to the naked eye. The results cast fresh light onto this artefact

class and open innovative investigative doors to establish a palette of pigments associated with polychromy on glass.

First, it is useful to summarise associated chronological, technological [1] and material developments and changes over time to situate our Vindolanda vessel into the context of glassmaking traditions.

Following its invention in the third millennium BCE in Iraq and northern Syria [2] (36.65), glassmaking technology spread to Egypt around 1500 BCE, where it was typically formed into artefacts through core-forming, casting, grinding and cold-cutting [3,4]. The development of the Hellenistic glass industry by the second century BCE saw glass formed into cast and slumped vessels [3], then rod-cutting for mosaic vessels by the mid-second century BCE [5].

There is some evidence for early prototype tube-blown vessels in the mid-first century BCE in the Eastern Mediterranean [6], but this technology appears to have taken some time to spread and a firm timeline for its development remains elusive. By the first quarter of the first century, fused bands of glass (with gold) were being inflated with a blowing iron, and small blown flasks and bottles were being produced in the Eastern and Western provinces while mould-blown vessels were introduced there between 25–40 CE, along with the expansion of free-blown vessel types [4,7,8].

By the mid-first century, Roman glassware was typically produced by the controlled blowing of melted glass through a pipe that was then formed into the required shape or, alternatively, mould-blown into a ceramic mould that was then manipulated [3,9,10]. Sometimes, these moulds contained manufacturers' brands, decorative motifs, texts or active scenes articulated in relief, including depictions of gladiatorial combat and charioteer games dating from c. 50–80 CE described by Pliny the Elder [2] (37.63–64), such as an exquisite example from Colchester, now in the British Museum collections, depicting gladiatorial scenes [11]. Blowing had a transformative impact on glassmaking, prompting the large-scale manufacture of an easily produced and diverse range of glassware vessels that were more accessible, affordable and, consequently, attractive to Roman consumers from across the full spectrum of society. This led to the establishment of a robust and profitable glass industry from the late first century [5], and colourless glass for fine tableware was popular from the late first to late third centuries [12] (p. 16), as seen in Figure 1.

Glass Making: A Timeline

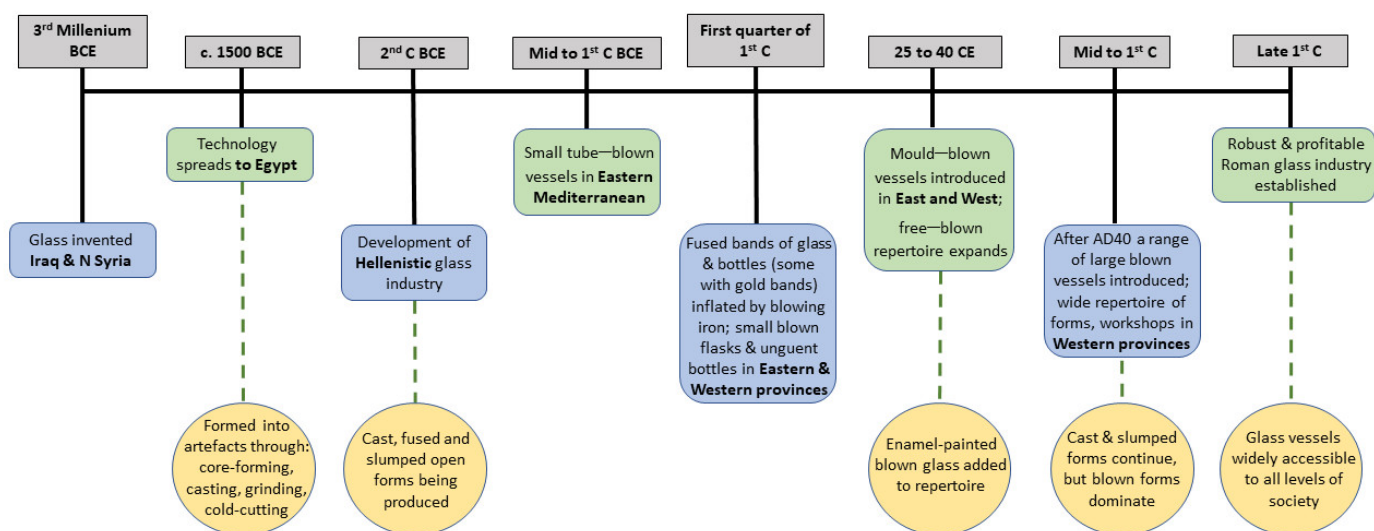


Figure 1. Timeline for glassmaking until the first century CE.

As a relatively homogeneous soda-lime-silica glass [13], the combination of the raw materials used (alkalis, calcium and silica), and their process of interaction during manufacture, meant that Roman glass could be produced at a reduced melting temperature of c. 1100–1200 °C [14]. Because of the ingredients used in its production, including calcium and aluminium, the chemical durability of glass ensures it survives extremely well, if generally fragmentarily, in the archaeological record. The melting process can impact the survival of elemental concentrations, a situation that can be exacerbated by the mixing of raw materials through recycling 25–40 [15].

Roman glassware was produced from silica sand and natron ($\text{Na}_2\text{CO}_3 \cdot 10\text{H}_2\text{O}$) or trona ($\text{Na}_2\text{CO}_3 \cdot \text{NaHCO}_3 \cdot 2\text{H}_2\text{O}$), relatively pure crystalline minerals comprising mainly sodium compounds [16]. Lime, or calcium oxide, acted as a stabiliser and calcium could originate from shell fragments in the natron or from the deliberate addition of plant ash, bone or limestone [14]. Effective glass production, then, requires a mineral soda source and calcareous sand with some variation between elements (e.g., Ca, Al, Fe and Ti) related to different minerals naturally occurring in the sands used, such as clays and feldspars [17]. Its composition typically includes low levels of Mn and K [18], so elevated levels of these two elements can indicate the use of sodium-rich plant ashes as fluxing agents [14,19], while elevated Pb and transitional metals, such as Co and Zn, may indicate the inclusion of recycled glass [17].

Glass may have been manufactured at high volumes as a raw product before being traded in blocks for the creation of various goods across the Empire [20]. Evidence for the production process remains elusive and contested, largely due to the ephemeral character of raw materials and the potential for different stages of production being undertaken in different locations [2,21] (36.193). Glass manufacture was, and remains, a highly skilled craft requiring a complex sequence of steps and intimate understanding of the properties of raw materials and management of their behaviour, as well as furnace conditions at various stages in the process.

The blue-green colour common to many Roman glasses derives from iron impurities naturally present in the sand used [12]. Calcining the iron-containing materials prior to

melting could decolourise the product, but using sand with high-purity and low iron produced consistently colourless glass [16]. Sand from areas such as the River Volturno were highly regarded for the manufacture of colourless products [2] (36.65). Indeed, Pliny states that “the most highly valued glass is colourless and transparent, as closely as possible resembling rock-crystal” [2] (36.200).

Decolourisation could also be achieved through the deliberate addition of decolourising agents, such as the minerals antimony (Sb) and manganese (Mn), to oxidise iron (FeO) impurities [22], resulting in a more yellow-green glass (Fe₂O₃) [1]. Antimony-based opacifiers (lead antimonate yellow and calcium antimonate white) were used as decolourants since the inception of glass production [23], aside from a brief interlude during the second and first centuries BCE where they were mixed with tin-based opacifiers (lead stannate yellow and tin oxide white) for glass beads in Britain, France [24,25] and Czechoslovakia [26]. That practice continued in glasses produced in Scotland from the second to first centuries CE [24]. By the first century, all Roman glass production used antimony-based opacifiers and had replaced tin-based products in Britain and France [25], a situation that was reversed during the fourth century where tin-based agents replaced antimony from the eastern Mediterranean to northern Europe [23]. It is possible for Mn to be introduced as contaminants to raw materials, e.g., present in Egyptian soils and sands [27], but this is unlikely for Sb which is not naturally present in the raw materials used in glass manufacture [16].

Elevated levels of Sb and/or Mn above trace levels present in colourless glass, therefore, suggest their deliberate addition as decolourising agents [28–30]. Although the mixing of both is generally thought to be primarily restricted to western provinces, including Britain and the Netherlands, which may be the result of recycling [15,28], recent evidence has also identified this previously unknown practice in Roman glass vessels from Egypt [9]. The incorporation of either Sb oxide (Sb₂O₅) or Mn oxide (MnO) for oxidation, then, varied across time and space [31]. Concentration levels of silica, lime (calcium oxide) and chlorine can inform colouration processes, but different levels of lead in yellows may be suggestive of workshops in diverse geographic locations, e.g., Egypt or Italy [30].

By the second and third centuries, Roman glass was composed of low levels of Fe, P and Ti, suggesting a refined industry selecting sands of high purity along with the deliberate inclusion of Sb and Mn decolourants for the production of high-quality colourless glass, perhaps in different centres of production than those manufacturing earlier blue-green glass from sands with lower purity [21]. By the fourth century, high iron, manganese and titanium glass (HIMT) originating from Egypt became increasingly common [19].

2. Roman Enamelled Glassware

A highly sophisticated, and largely unexplored, class of Roman glassware is decorated with coloured enamelling, a technique that has been used from as early as the fifteenth century BCE in Mediterranean and Eastern civilizations [32–34]. Enamel is created by mixing pigments with a binder then painted onto a vessel and fused into place by re-firing [35]. Two glass enamelling methods are known: pre-melted, comprising a mixture of pulverised coloured glass compatible with the base vessel with a liquid medium (e.g., water and gum Arabic); and cold-mixed, comprising a colourless glass similar to, or the same as, the base vessel pulverised and mixed with a liquid medium and colouring agent, e.g., metallic oxide such as cobalt oxide for blue enamel or coloured minerals including hematite to create red [36], as shown in Figure 2.

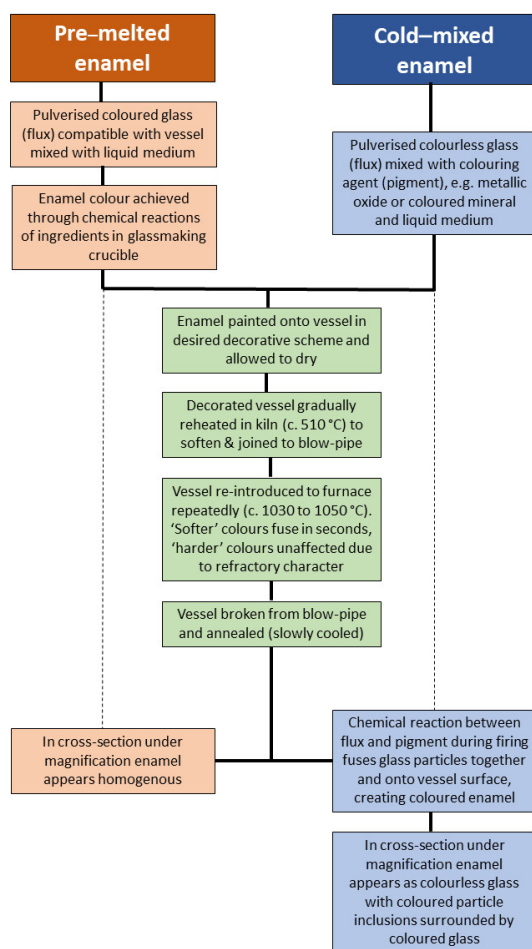


Figure 2. Glass enamelling process (information summarised from [36,37]).

Surviving examples of enamel-painted Roman glass drinking vessels are vanishingly rare, as exemplified by the unique and beautifully articulated scenes of a gladiatorial battle painted onto the fragile fragments of a drinking vessel recovered from Vindolanda, a Roman fort just south of Hadrian's Wall. This is a cylindrical cup with a fire-rounded rim and (missing) double base ring produced in the late second century and first half of the third century [12] (pp. 99–101, Figure 37). It finds some stylistic and chronological parallels with enamel-painted glass beakers from burial contexts in Denmark, thought to have been manufactured at Cologne, lower Rhineland [38–40]; Zaborów, Western Mazowsze, Poland [41]; and Lubieszewo, Poland [42], known as the Lübsow beakers. Some of these vessel types were enamel-painted with similar scenes from the arena and decorative dots such as the Vindolanda vessel. A small number of fragments from this high-end body of material have been recovered from Britain [12,43] (pp. 100–101).

Earlier tall conical enamelled beakers painted with gladiatorial and other scenes recovered from Begram, Afghanistan [44,45] date from the first century; see Figure 3, top right. Another group of glass cup fragments from Masada, dating to the first century, commonly referred to as Hofheim cups or beakers [12] (pp. 71–73, Figure 21), also depict gladiatorial combat. They are thought to be the earliest examples of this thematic content, but are poorly preserved and enamelled onto semi-transparent dark cobalt blue glass [46]. Another extraordinarily well-preserved transparent green Hofheim cup decorated with very similar vibrant colours to the Vindolanda vessel, but depicting fauna and birds, was discovered in the Locarno cemetery in Switzerland and thought to have been created in a Syrian or a northern Italian workshop during the first century [36], as seen in Figure 3.



Figure 3. The Locarno vessel (image © Mark Taylor, used with permission).

Roman glass enamelling has received only very limited scholarly attention, primarily focused on the addition of colourants and opacifiers to a base glass [47] and the common characteristics of certain colours on opaque and translucent glasses [48]; see Table 1. Helpful tabular summaries of known first century enamelled vessels and summaries of some historic pigments are available [46,49], but there remains a gap in knowledge on the diversity and properties of the pigments potentially used in the enamelling process. Experimental work using crushed coloured glass has shown that during enamelling firing, darker colours categorised as ‘softer’ [36] shine within seconds, confirming they have fused, while the more refractory character of lighter, ‘harder’, colours, e.g., yellow and red, are less affected by the heat. This introduces an additional layer of complexity to the production process of vessels decorated with different colours to manage variable reactions and prevent the vessel’s collapse during repeated withdrawals from the furnace while remaining attached to the blowpipe, or pontil in the case of vessels with fire-polished rims [37]. Visible differences are also discernible with ‘softer’ colours appearing thin and fluid in character, and a slight sinking or bulging of the vessel glass below, while the ‘harder’ refractory colours present with a grainy appearance that signifies less firing time [36]. The ability to control these variables is a testament to the extraordinary skills of the artisans creating iconic enamelled glassware.

A close microscopic inspection of the Vindolanda vessel reveals that these characteristics are present with a granular surface on cream and yellow (harder) colours, and pigment particle micro-crystallites are clearly discernible in red and blue features (contra. [49] (pp. 90)) as well as in some yellows. Like the Masada gladiator glass [46], the Vindolanda vessel scenes were created by the freehand application of outlines which were then filled in with coloured enamelling agents, and the outlines visibly survive in some areas, especially features depicted in blue and red. The enamel surfaces suggest they were prepared through cold-mixing [36], rather than the pre-melting of coloured glasses [47].

Table 1. Common, known, colourants in Roman pre-melted enamels (information summarised from [37,46,48,50]).

Enamel Colour	Opaque	Translucent (Metals in Solution)
Black	Commonly very dark translucent olive-green glass or possibly combinations of cobalt oxide (CoO), iron oxide (Fe ₂ O ₃), copper oxide (Cu ₂ O) and/or manganese dioxide (MnO ₂)	Iron (Fe)
Blue	Cobalt oxide (CoO)	Copper oxide (Cu ₂ O) OR Lapis lazuli (Na ₇ Al ₆ Si ₆ O ₂₄ S ₃)
Blue (Dark)	Commonly translucent glass with added calcium antimonate (CaSb ₂ O ₆)	Cobalt (Co)
Blue-green	Commonly translucent glass with added calcium antimonate (CaSb ₂ O ₆)	Copper (Cu) or iron (Fe)
Brown	Iron oxide—hematite (Fe ₂ O ₃)	Manganese dioxide (MnO ₂)
Brown (golden)	-	Manganese (Mn)
Orange	Cuprous oxide (Cu ₂ O)	-
Green	Commonly translucent glass with added lead antimonate (Pb ₂ Sb ₂ O ₇) Alternatively, decayed reds or oranges Alternatively, lead antimonate (Pb ₂ Sb ₂ O ₇) with added lapis lazuli (Na ₇ Al ₆ Si ₆ O ₂₄ S ₃)	Iron (Fe), or copper (Cu)—in lead (Pb)-rich glass
Green (pale)	Iron oxide (Fe ₂ O ₃)	Copper oxide (Cu ₂ O) with iron oxide (Fe ₂ O ₃)
Pink	-	Manganese dioxide (MnO ₂)
Purple	-	Manganese (Mn)
Red	Iron oxide -hematite (Fe ₂ O ₃); Copper (Cu) or cuprous oxide (Cu ₂ O)	-
Yellow	Lead antimonate (Pb ₂ Sb ₂ O ₇)	-
White	Calcium antimonate (CaSb ₂ O ₆)	-

3. Heritage Materials Science Technique

So rare are these vessel-types that they have received very limited attention and they have never been subjected to pXRF analysis, although a small number have been investigated using lab-based μ -Raman and μ -XRF [40,51] and portable Raman spectroscopy [50].

Traditionally, the capture of the comprehensive chemical composition of heritage glass has been undertaken through the deployment of laboratory-based instruments that are, by their very nature, destructive analytical techniques. These include Laser-ablation Inductively-Coupled-Plasma Mass-Spectrometry (LA-ICP-MS) [52]; Fast Neutron Activation Analysis (FNAA) [53]; X-Ray Fluorescence (XRF) [54]; Raman Spectroscopy [55]; Ion-Beam Analysis, including Particle Induced X-Ray Emission (PIXE) and Particle (proton) Induced Gamma Emission (PIGE) [56,57]; Isotope-Ratio Techniques [17]; X-Ray Powdered Diffractometry (XRPD) and Electron Probe Microanalysis (EPMA) [58] and Scanning Electron Microscopy (SEM) [59]. The latter technique is not in-and-of-itself an invasive procedure, but it does necessitate the movement of curated artefacts out of the relative safety of museum stores and is suitable only for smaller, portable artefacts, or the destructive extraction of samples.

Largely due to the availability of relatively reasonably priced instrumentation, portable techniques now permit analysts to exploit the latent research potential of precious curated collections without risk to their integrity. As a result, the application of *in situ* non-invasive analytical techniques in the field of heritage materials science has grown exponentially in recent years. PXRF and other analytical technologies [60], including Raman spectroscopy [50], Multi Spectral Imaging (MSI) [61,62] and Spectral Imaging [63], now make it possible to characterise materials used in the creation of some of the most exquisite artefacts from Antiquity, including Roman glass.

Most studies are commonly restricted to the classification and identification of the colourants, decolourants, opacifiers and other ingredients used in the glass production process for vessels and tesserae [9,18,64,65]. However, there remain gaps in our understanding of changes across time and place [17], and highly specialised products, such as

strongly coloured mosaic [30] and enamel-painted glass vessels that most likely remained accessible only to the upper echelons of Roman society, are particularly underexplored.

Portable XRF has been successfully deployed to characterise the enamelling used in the creation of seventeenth–eighteenth century enamelled French watches in the collections of the Musée du Louvre in Paris [66]. In the absence of any comparable investigation for Roman enamel-painted glass, this vanguard research seeks to test the potential of pXRF as an analytical tool for the analysis of this class of material to determine whether the different enamelling technologies and pigments used in their manufacture can be established.

4. The Vindolanda Vessel

The remains of a unique and beautifully preserved enamel-painted colourless drinking glass from Vindolanda that may have originated from the Rhineland [67] comprise four adjoining fragments recovered from different locations across the site over three seasons of excavation between 1972 and 2007 (Figure 4). Contexts include an alleyway between two extramural buildings opposite the south-western corner of the fort (artefact no. 711); a small pit adjacent to an oven in a tavern from the third century extramural settlement outside the west gate of the fort (artefact no. 5454); and from silt near the base of the western fort ditch (artefact no. 11078) [68]. Aside from 711, a small body sherd that adjoins 11078, the fragments form a near-complete straight-sided vessel with the beginning of a curved base. The diagnostic base is missing, which makes a definitive identification challenging, but the shape conforms to thin-walled cylindrical beakers categorised as Isling 85B dating from the late second to first half of the third century [69].

These fragments have been refitted to reveal an exquisitely executed, vibrant and colourful scene of gladiatorial combat (Figure 5) with four officials and three gladiators, two of whom are actively engaged in combat, flanked on either side by officials. This is a scene and theme commonly represented across several media, including a recently discovered Pompeiian fresco, *terra sigillata*, colour-coated wares, terracotta flasks, lamps and other glassware (see Figure 6 for examples in glass).

The combatant on the left two adjoining fragments (artefact no. 5454) is depicted in the classic regalia of a *Secutor* (pursuer) and adopting an offensive stance leading with his left arm and foot. He wears a short dark brown tunic/loincloth (*subligaculum*) trimmed at the top of the thighs and waist in cream with light brown leather belt (*balteus* or *cigulum*), and his right foot is covered with a yellow boot decorated with a brown area on the shin and underfoot. For protection, he wears a smooth colourful *galea* (plumed helmet with visor and small eye holes) topped in red with blue faceguard trimmed in yellow; a *manica* (leather elbow and wrist guard) covering his right arm with creamy-yellow interior, dark brown exterior and dark brown/black padding on the elbow and shoulder guard depicted in dark blue with lighter blue diagonal stripe in the centre. In his left hand, he holds a large cream *scutum* (shield) decorated in brown lines with a very dark brown boss and a thick padded cream *ocrea* (shin guard) strapped onto his left shin with a dark central area which suggests a different material, possibly bronze, for greater protection here. He is equipped with a *gladius* (short sword) with blue blade (faded) and red pommel held in the right hand ready to thrust at his opponent.



Figure 4. The Vindolanda gladiator enamel-painted vessel fragments ((top): 5454; (bottom): 11078 and 711).

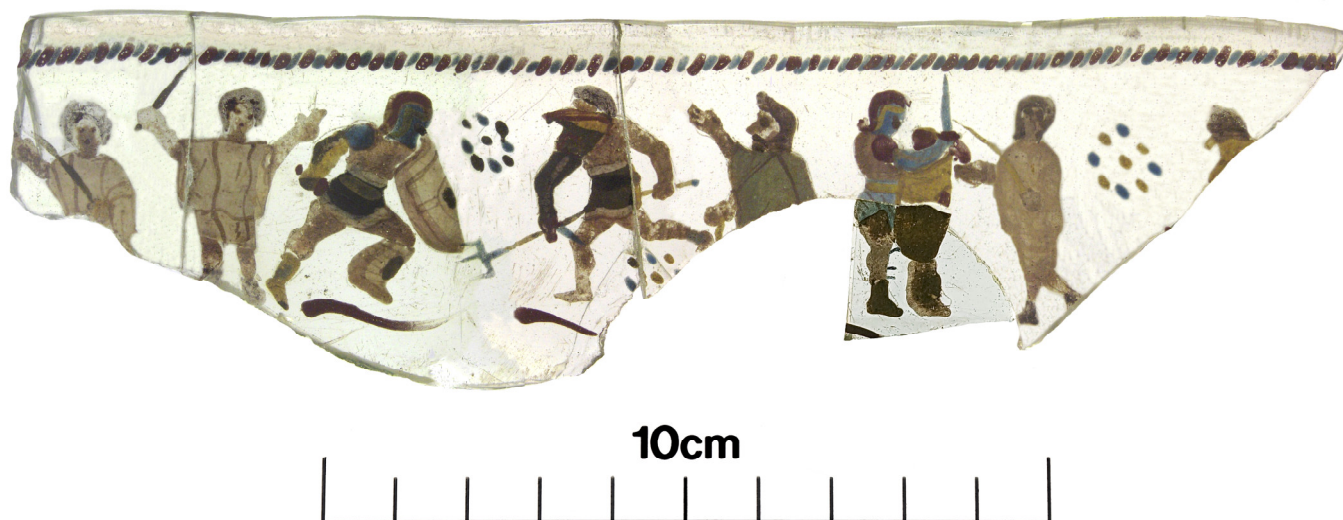


Figure 5. Flattened image of the Vindolanda Vessel (© Barbara Birley, used with permission).



Figure 6. Representations of gladiators on Roman glassware—(A) First C blue moulded glass cup with combatant names inscribed above, Musée gallo-romain de Fourvière, Lyon; (B) First C enamel-painted beaker from Begram, Afghanistan, Guimet Museum, Paris; (C) Third C drop-flasks in the form of a *Secutor* helmet with “snake-thread” trails made in Rhineland, British Museum; and (D) Romisch-Germnisches Museum, Cologne. All images used with permission [70].

His opponent (artefact nos. 5454 and 11078) is a *Retiarius* (net man) equipped with weapons inspired by the tools of fishermen, also depicted in an offensive stance leading with his left foot mirroring his adversary. He wears a light brown tunic (*subligaculum*) with a dark belt (*balteus* or *cigulum*), also trimmed at the top and bottom with cream, and unlike the *Secutor*, he is not protected by a *scutum*, *galea* or *ocrea*. Instead, his only protection is a dark brown *manica* defined with a cream central line on his left arm topped with a yellow *galerus* (metal shoulder piece) with red detail that covers the left side of his bare face and head. His only weapons are a *pugio* (dagger) in his left hand which he uses to hold steady the front of a *fascina* (long, three-pronged trident) with yellow shaft and blue prongs used to stab at or throw at opponents. The *rete* (weighted net) which would normally be part of his repertoire and used to entangle opponents is not depicted in this scene, presumably because it is too challenging to define on such a small and delicate vessel.

Three of the officials are clean-shaven and dressed in cream tunics with brown vertical stripes and hold official wands depicted in yellow in their left hands while giving signals to the combatants with their right. They are referees or *lanistae*, owners of *ludi* (gladiator schools) [71] (pp. 166). The fourth, on the right of the *Retiarius*, has a beard and wears a bluish tunic and may be judging the bout or perhaps is the *editor* (rich sponsor of the event). The scene is mirrored in other contexts, including the spectacular mosaic at a Roman villa in Nennig, near Treves in Germany (Figure 7).



Figure 7. Third Century CE mosaic from the Roman villa at Nennig depicting a *Retiarius* versus a *Secutor*. Image used with permission [70].

The third gladiator is preparing for battle (artefact no. 11078), awaiting his turn in the next bout and overseen by a *lanista*. He also appears to be a *Secutor*, though the colours of his garments and equipment are very different to the one discussed above. He wears a blue loincloth and a yellow belt, and a blue *manica* with a red shoulder guard and carries a *gladius* with a blue blade and red pommel. The interior of his *scutum* is a bright, vibrant red, as is the pommel of the *gladius* raised aloft in his right hand, depicted with a blue blade. His legs and *scutum* base (artefact no. 711) differ markedly from other features since taphonomic processes have discoloured the pigments to dark brown, which makes it challenging to depict features, though they are visible in the vessel interior. It is quite possible the *lanista* on the extreme left of the vessel is similarly preparing his opponent, probably a *Retiarius*, for the next bout, but the combatant is missing from the scene since the final piece of this glass jigsaw remains undiscovered.

5. Methodology

5.1. Portable X-Ray Fluorescence (pXRF)

pXRF is commonly used to characterise the colourants, opacifiers and impurities present in the manufacture of glass [72,73] on tesserae [65] or mosaic glass vessels [30]. There are, however, limitations and weaknesses inherent in the technique that must be considered when deploying pXRF as an effective diagnostic tool, a situation that is somewhat exacerbated by the complex and diverse materials used in the manufacture of heritage glass [74]. That said, taking an analysis spot on an unpainted area of the glass vessel provides ground data that serves to mitigate these issues and differentiate between the materials used in the vessel's manufacture and the elemental composition of enamelling materials.

In situ Non-invasive pXRF and microphotography were deployed for detailed surface examination and to characterise the elemental compositions of pigments on each painted feature. The pXRF instrument used was an Olympus Vanta M Series (VMR-CCC-G2-K) hand-held analyser with rhodium anode in 4-W X-Ray tube capable of voltage up to 50 kV. The instrument operates with two beams: one at 10 kV and one at 50 kV. Analyses were undertaken in the GeoChem (G2) mode where the X-Ray tube operated at 40 kV and ~70 μ A to measure heavier elements and at 10 kV and ~90 μ A to measure lighter

elements. The measurement time was 30 s: 10 s for the heavier elements and 20 s for the lighter elements, and the area of analysis was 7.069 mm². Several of the forty elements from Mg to U that the instrument can detect were present below the limit of detection (LoD), and light elements with fluorescent peaks at low energies were poorly resolved at low concentrations.

A total of fifty-two analysis spots were captured across the fragments: twenty-seven on artefact number 5454 (Figure 8, top), including one ground on an unpainted area of glass, twenty-two on artefact number 11078 and three on artefact number 711 (Figure 8, bottom). Sample spots are grouped according to artefact number and summarised in Table 2, and composition tables comprising the full dataset are provided in Supplementary Materials while the concentrations of each main element associated with the pigments are provided in Table 3. The elements related to each painted feature are discussed in-text. Elemental concentrations are expressed in parts per million (ppm). Some elements, including Rb, Sr and Zr, have been excluded from the broader discussion on analysis as occurring through the glass manufacture process, confirmed by the ground analysis spot where no pigments were applied. The remaining 22 elements provided a level of quantification at various spots in concentrations sufficiently above background levels to confidently identify the pigments present, although some only at low trace levels. Samples were taken from as many features as possible to compare results and colours, although no samples were taken on the tunics of the three *lanistae* since the pigment appeared to visibly correlate with that on the *scutum* of both *Secutores*.



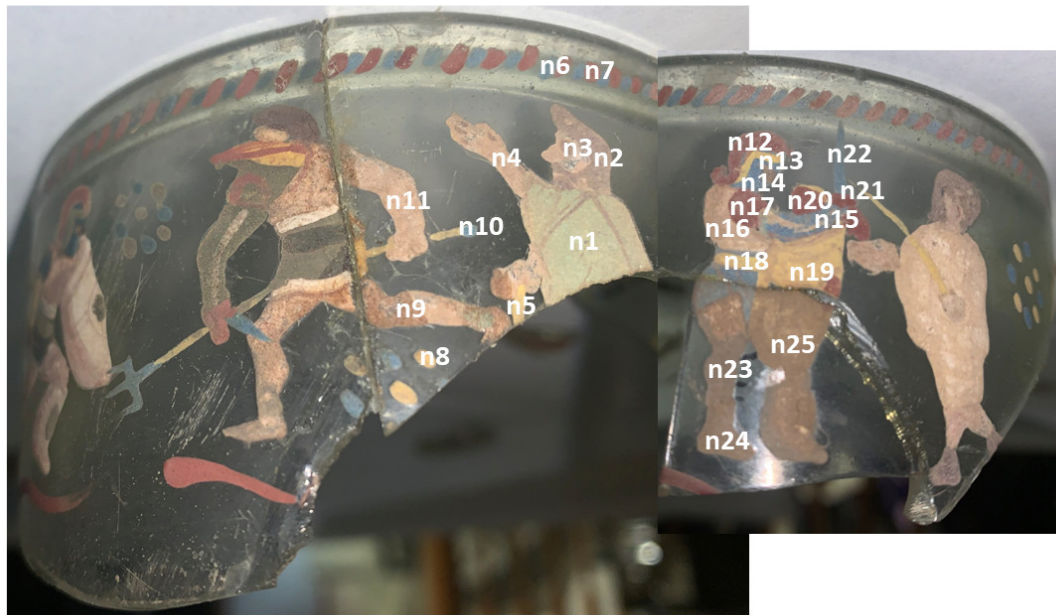
11078
& 711

Figure 8. pXRF analysis spots on artefact nos. (top) 5454 and (bottom) 11078 and 711.

Table 2 records the locations of the samples analysed by pXRF on Artefact No. 5454 depicting the *Secutor* and *Retiarius* battle scene and two *lanistae*; and Artefact Nos. 11078 and 711 depicting a *Secutor* preparing for a bout, a judge/editor? and a *lanista* indicated by an 'n' prefixing sample number.

Table 2. Locations of pXRF analysis spots on artefact nos. 5454, 11078 and 711.

Sample	Feature	Colour/s
Artefact No. 5454		
1	<i>Retiarius</i> helmet	Brown/red
2	<i>Retiarius</i> facemask	Red
3	<i>Retiarius</i> facemask	Brown
4	<i>Retiarius</i> manica	Brown
5	<i>Retiarius</i> pugio pommel	Red
6	<i>Retiarius</i> pugio blade (possible leg interference)	Blue
7	<i>Retiarius</i> thigh	Beige (skintone)
8	<i>Retiarius</i> subligaculum centre	Light Brown
9	<i>Retiarius</i> balteus/cigulum	Dark Brown
10	<i>Secutor</i> scutum	Cream
11	<i>Secutor</i> scutum boss	Dark brown
12	<i>Secutor</i> subligaculum bottom trimming	Cream
13	<i>Secutor</i> balteus/cigulum	Yellowish
14	<i>Secutor</i> chest	Beige (skintone)
15	<i>Secutor</i> galea facemask	Blue
16	<i>Secutor</i> galea facemask	Yellow
17	<i>Secutor</i> galea	Red
18	<i>Secutor</i> manica front	Yellow
19	<i>Secutor</i> manica elbow	Brown
20	<i>Secutor</i> manica shoulder guard (exterior)	Dark Blue
21	<i>Secutor</i> manica shoulder guard (central diagonal stripe)	Light Blue
22	<i>Secutor</i> boot base	Yellow
23	<i>Secutor</i> boot centre	Brown

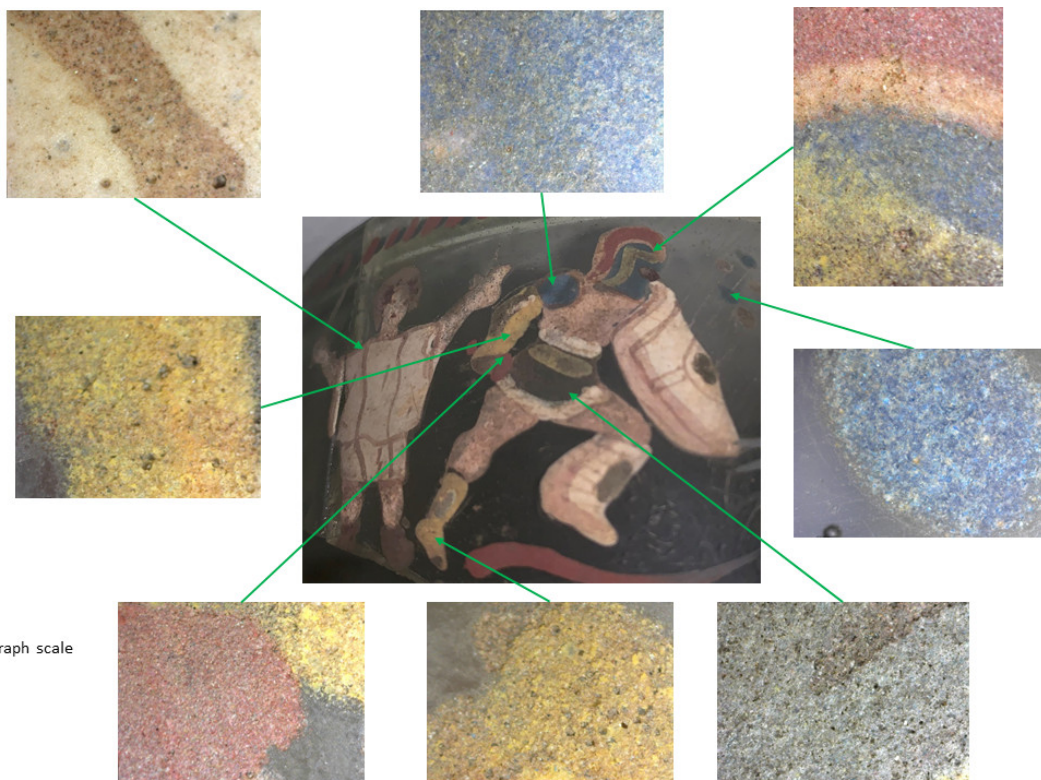
24	<i>Retiarius fascina</i> central prong	Blue
25	<i>Retiarius fascina</i> shaft	Yellow
27	Decorated band under <i>Retiarius</i>	Red
26	Ground—plain, unpainted glass	Colourless
Artefact Nos. 11078 and 711		
n1	Judge/editor? tunic	Blue
n2	Judge/editor? hair	Brown
n3	Judge/editor? eye	Dark Brown
n4	Judge/editor? forearm	Beige (skintone)
n5	Judge/editor? wand	Yellow
n6	Decorative dot	Blue
n7	Decorative dot	Brown
n8	Decorative dot	Yellow
n9	<i>Retiarius</i> knee guard	Brown
n10	<i>Retiarius' fascina</i> terminal	Blue
n11	<i>Retiarius</i> forearm	Beige (skintone)
n12	<i>Secutor</i> helmet	Brown
n13	<i>Secutor</i> facemask (possible interference from blue area)	Yellow
n14	<i>Secutor</i> facemask	Blue
n15	<i>Secutor manica</i>	Blue
n16	<i>Secutor</i> torso	Beige (skintone)
n17	<i>Secutor manica</i> shoulder guard	Brown
n18	<i>Secutor balteus/cigulum</i>	Yellow
n19	<i>Secutor scutum</i> front	Yellow-cream
n20	<i>Secutor scutum</i> —inner top	Red
n21	<i>Secutor gladius</i> pommel	Red
n22	<i>Secutor gladius</i> blade	Blue
n23	<i>Secutor</i> knee	Brown
n24	<i>Secutor</i> boot	Brown
n25	<i>Secutor scutum</i>	Brown

5.2. Microphotography

Surface examination at the visible and microscopic level of surviving pigments is fundamental for providing a comprehensive review of their condition and for revealing similarities or differences between painted features. Given the fragile character of the glass vessel and the likelihood that the pigments have been affixed to the exterior then re-fired in a kiln, it was not possible to extract microsamples for Light Microscopy or other laboratory-based analytical techniques. *In-situ* digital microphotography was, therefore, captured using a Dino-Lite Edge Digital Microscope (AM4515ZT) which provided powerful high-resolution images for detailed surface inspection (Figure 9). Dino-Lite instruments have been used to great effect for portable microscopy and image capture for a diverse range of archaeological artefacts including textiles [75], pigments on Classical statuary [60], metallurgy [76], ceramics [77], lithics [78], bone tools [79] and even close-range photogrammetry [80].

The Dino-Lite microscope was connected by USB to a Microsoft Surface Pro 7+ tablet with Intel Core i7 1165G7, Windows 10, Iris Xe Graphics, 16 GB RAM and 256 GB SSD, 12.3" touchscreen installed with DinoCapture 2.0 software which controlled illumination and exposure, viewing, export and measurements. This model has adjustable 20–220× magnification, flexible LED control (FLC), integrated adjustable polarizer, Automatic Magnification Reading (AMR) and a 1.3 Megapixel Edge sensor. Images were acquired at the highest resolution of 1.3 megapixels (1024 × 1280 pixels) and a colour depth of eight-bit using the DinoCapture software, before being exported as JPEGs.

A



B

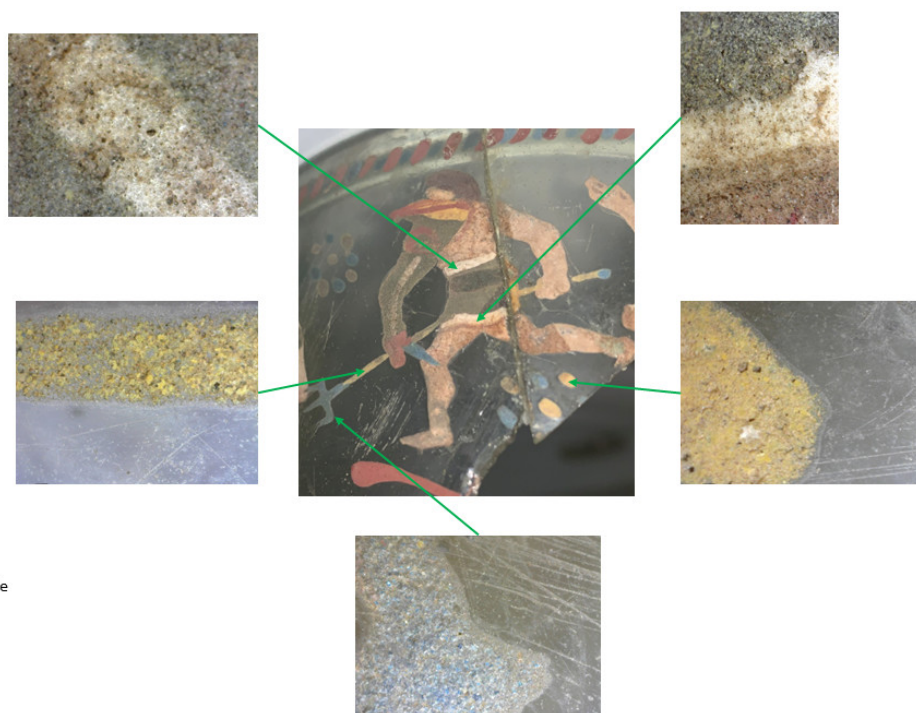




Figure 9. Microphotographs of pigments depicting features on the *Secutor* on artefact no. 5454 (A); *Retiarius* on artefact nos. 5454 and 11078 (B); *Judge/Editor?* on artefact No. 11078 (C); and *Secutor* on artefact nos. 11078 and 711 (D).

6. Results

The concentrations of each main element related to the pigments are provided in Table 3 and the full dataset is provided in Supplementary Materials. Given the variety of features depicted with different enamels across the Vindolanda vessel, it is helpful to provide a summary of the notable points relating to each element and some observations in Table 4.

Table 3. Concentrations of main elements identified by pXRF (displayed as ppm), <LOD is below Limit of Detection.

Sample	Colour	Mg	Al	P	S	K	Ca	Fe	Co	Cu	As	Sb	Hg	Pb
26	Colourless (ground)	<LOD	10,157	<LOD	860	962	32,036	3528	<LOD	57	16	3653	<LOD	120
n12	red	<LOD	3833	187	<LOD	442	22,201	22,562	<LOD	1270	153	5124	<LOD	753
n20	red	<LOD	8558	831	5542	1729	16,613	31,627	<LOD	2694	1504	5867	<LOD	16,397
n21	red	<LOD	10,194	1203	2031	1856	21,488	47,757	<LOD	5562	295	5320	<LOD	1966
2	red	<LOD	12,718	2363	10,592	1991	17,664	26,905	<LOD	413	1834	4595	<LOD	12,565
5	red	<LOD	11,242	1821	8498	1590	21,703	31,227	<LOD	6530	703	4507	<LOD	4459
17	red	<LOD	8650	2101	2465	2056	23,855	36,506	<LOD	1580	82	4473	<LOD	821
27	red	<LOD	10,504	2070	3459	927	19,062	59,304	<LOD	1109	146	3892	13	821
n2	brown	<LOD	13,668	1207	291	1703	20,057	30,011	<LOD	206	42	4152	12	255
n3	brown (dark)	<LOD	17,292	2086	284	2286	11,659	53,968	<LOD	375	80	4589	<LOD	488
n7	brown	<LOD	4530	<LOD	345	428	21,635	20,817	<LOD	4777	99	5197	29	678
n9	brown	23,447	22,425	1810	2037	1272	17,664	13,749	<LOD	193	32	3714	<LOD	213
n17	brown	<LOD	19,724	1619	1214	2078	18,615	49,905	<LOD	2147	90	4610	<LOD	853
n23	brown	13,352	28,441	5070	2926	6297	23,281	7605	<LOD	182	88	3447	<LOD	327
n24	brown	<LOD	21,756	2834	6123	4201	13,764	9127	<LOD	240	2189	4263	<LOD	15,015
n25	brown	<LOD	16,288	3099	11,575	4338	9827	8119	<LOD	363	4450	7778	<LOD	40,549
1	brown	<LOD	22,139	9014	7955	2401	16,571	50,660	<LOD	464	242	4246	<LOD	1159
3	brown	<LOD	11,729	2496	36,060	1364	11,551	14,553	<LOD	767	5715	7127	<LOD	46,865
4	brown	<LOD	12,236	3184	16,760	1332	17,364	12,927	<LOD	16,953	1348	5154	<LOD	11,495
8	brown (mid)	17,440	11,761	2124	40,961	580	8061	5542	<LOD	934	6293	7762	<LOD	54,009
9	brown (dark)	<LOD	8266	1941	18,832	1015	20,428	15,504	<LOD	21,480	1358	7630	<LOD	40,340
11	brown (dark)	<LOD	10,781	1877	6447	1197	27,506	6076	<LOD	4038	95	3999	<LOD	474
19	brown	<LOD	9139	2955	22,894	735	12,971	5131	<LOD	537	4193	6155	<LOD	30,275
23	brown	<LOD	12,999	4789	10,412	981	18,048	4291	<LOD	3313	2144	5154	<LOD	17,831
n4	fleshtone	<LOD	3815	<LOD	<LOD	711	21,766	12,164	<LOD	400	129	4283	<LOD	379
n11	fleshtone	34,323	17,071	1044	1613	1096	20,512	17,802	<LOD	231	47	4059	<LOD	301
n16	fleshtone	<LOD	<LOD	<LOD	<LOD	<LOD	10,091	26,010	<LOD	4293	761	8689	<LOD	8448
7	fleshtone	13,209	17,949	7316	5647	1750	21,632	12,716	<LOD	574	93	3635	<LOD	677
14	fleshtone	<LOD	13,675	7030	3266	1901	23,663	21,062	<LOD	837	130	3842	<LOD	495
10	cream	<LOD	9269	1577	2542	<LOD	25,627	4332	<LOD	246	133	3631	<LOD	522
12	cream-white	<LOD	12,548	3835	5187	<LOD	23,964	12,861	<LOD	7581	135	4138	<LOD	1324
n1	blue	<LOD	16,801	788	7869	1550	18,897	7488	<LOD	12,432	1717	5062	<LOD	10,790
n6	blue	<LOD	<LOD	<LOD	<LOD	<LOD	25,136	13,150	<LOD	2354	57	4825	<LOD	352
n10	blue	<LOD	6453	249	1962	924	31,400	4106	97	3105	150	4147	<LOD	1227
n14	blue	<LOD	<LOD	<LOD	<LOD	<LOD	19,249	8734	<LOD	2166	328	6836	<LOD	1741
n15	blue	<LOD	<LOD	<LOD	<LOD	<LOD	13,103	10,433	<LOD	123	127	6609	<LOD	629
n22	blue	10,096	8657	569	1318	1415	31,592	4973	183	6818	154	4462	<LOD	849
6	blue	<LOD	8989	1363	5070	1479	30,326	7990	202	8616	260	4541	<LOD	2075
15	blue	<LOD	9186	2278	9022	1858	24,537	21,752	273	15,282	875	7040	<LOD	5197
20	blue (dark)	<LOD	10,241	4118	5095	2396	31,265	12,496	402	13,279	288	5762	13	1800
21	blue (light)	<LOD	7658	2215	3962	2206	32,639	8275	755	18,058	407	6784	<LOD	2743
24	blue	<LOD	13,197	1107	3404	1565	32,274	5705	257	10,179	188	4503	<LOD	1020
n5	yellow	<LOD	9527	588	4074	424	19,045	6117	<LOD	4689	792	4443	<LOD	6009
n8	yellow	<LOD	19,911	907	13,429	1831	18,391	5340	<LOD	283	2193	4092	27	15,369
n13	yellow	<LOD	<LOD	<LOD	<LOD	<LOD	17,406	12,514	<LOD	2777	<LOD	6748	<LOD	573
n18	yellow	<LOD	20,508	1497	9626	1715	19,830	8409	145	7033	1982	6013	<LOD	13,635

n19	yellow-cream	<LOD	14,120	924	18,462	1992	10,459	6519	<LOD	509	4866	7795	<LOD	48,470
13	yellowish	<LOD	9124	1668	20,578	<LOD	14,987	6787	<LOD	8738	2831	5225	65	17,526
16	yellow	<LOD	7874	1863	23,349	1228	17,804	11,303	185	10,412	3227	9415	<LOD	24,662
18	yellow	<LOD	7630	2393	11,890	904	21,080	6800	<LOD	709	1479	4656	<LOD	8822
22	yellow	<LOD	7872	1966	5120	844	25,019	3436	<LOD	472	833	3778	<LOD	7061
25	yellow	<LOD	14,692	1438	11,442	1550	25,989	3810	<LOD	499	636	3687	<LOD	2814

Table 4. Textual summary of elements as they relate to each enamel-painted feature.

Element	Note
Mg	below LOD on colourless glass, but very high on some brown samples, especially on the Retiarius knee guard and subligaculum centre non-combatant Secutor's knee and gladius blade (artefact 11078), and on the fleshtones of the Retiarius' forearm and thigh
Si	high level present in the colourless glass is overwhelmed by pigments on ALL painted areas
P	below LOD in colourless glass, but elevated in almost all samples, particularly high in the brown Retiarius galea and fleshtones of the thigh of the Retiarius and chest of the Secutor on artefact 5454
S	slightly elevated in the colourless glass, but high readings in most samples, especially the gladiatorial accoutrements, e.g., Retiarius' galerus and subligaculum where it is exceptionally high and his balteus/cigulum and manica; and the Secutor's manica elbow padding which is visibly a similar colour to the Retiarius's galerus and subligaculum, his scutum (in both the degraded area and yellowish area); and yellow areas of the 11078 Secutor's scutum, balteus/cigulum and galea facemask
K	relatively low in the colourless glass and elevated on many samples, especially in brown and red features and some blue spots, but particularly high in the areas where pigment is degraded on artefact 711 (could be salt crustation from post-depositional position)
Ca	as with Si, the high level present in the colourless glass is overwhelmed by pigments on almost all painted features, except those coloured with blue
Ti	trace levels in some features, e.g., brown judge/editor's eye, and degraded pigment on the Secutor's boot (artefact 711) and Retiarius' manica, as well as the fleshtone of the Secutor's torso and two shades of blue on the Secutor's manica shoulder guard; and the yellows of the Secutor on 11078 facemask (but the spot could have interference from the blue area here), and his balteus/cigulum and scutum
V	very low level on colourless glass and only trace levels on a few areas dispersed across samples with no consistent pattern to colours, except for fleshtones, where most samples have slightly elevated levels
Mn	present at low levels on the colourless glass and even lower on painted features
Cr	below LOD in colourless glass and trace levels from some samples, e.g., red on the Secutor's galea (5454) and browns in the Retiarius's accoutrements, including knee guard, galerus, manica and scutum boss; also on several blue samples, especially weapon blades, shoulder guards, decorative circle and judge/editor's tunic
Fe	only trace levels on the colourless glass but elevated on ALL samples except two yellow features, especially in all red and almost all brown samples and highest in areas where layered pigment is most likely (features painted on top of others), e.g., judge/editor's eye and hair, Secutor's manica shoulder guard, galea facemask and shoulder guard, Retiarius' galerus, manica and balteus/cigulum. Also high in fleshtone areas, especially the chests of both Secutores
Co	below LOD on colourless glass and elevated exclusively on blue areas as well as two slightly elevated yellow samples, both of which either overly or sit immediately beside blue features. Highest levels from the light and dark blue of the combatant Secutor's shoulder guard
Ni	below LOD on colourless glass with trace levels on a few blue samples, e.g., Secutor's galea facemask and two shades of blue in the Secutor's shoulder guard as well as the Retiarius' pugio blade. One elevated reading on a yellow sample likely derives from the blue on the combatant Secutor's galea facemask since the yellow has been visibly painted over a blue base here
Cu	very low trace level on colourless glass and elevated levels on almost all painted features, mostly at unremarkable levels, but high levels evident from all but one blue sample (Secutor's manica on 11078, which could suggest the analysis spot had interference from several coloured features here as most of the elements detected are anomalous with other blue samples), especially elevated at the judge/editor's tunic, and combatant Secutor's shoulder guard and galea facemask as well as the Retiarius' fascina prong. The highest levels of Cu on brown samples are from the Retiarius' manica and balteus/cigulum which may suggest mixing with blue on these features. One yellow sample has high Cu, at the Secutor's galea facemask, which likely derives from the blue feature here since the yellow has been visible painted over a blue base here

Zn	low trace levels on colourless glass and elevated in some spots, including the Retiarius' manica and balteus/cigulum aligning with the high Cu here as well as the blue spots aligning with high copper on the judge/editor? tunic, the Secutor's galea facemask and shoulder guard and also on the yellow spots of the Secutor galea facemask and balteus/cigulum. Again, it is visible evident these yellow features were painted over underlying colours in these areas
As	very low trace levels on colourless glass and elevated levels on many samples. For example, elevated on yellow features, especially the non-combatant Secutor's scutum front, galea facemask/balteus/cigulum as well as the decorative circle and manica front, and highest readings in some brown samples, e.g., Retiarius' subligaculum and galerus as well as the Secutor's boot and knee (degraded pigment on 711) and combatant Secutor's manica elbow pad and boot central feature. These correspond with the highest levels of pb, suggesting a mix or layer of arsenic and lead-based pigment or antimony, lots of black dots suggest antimony on microphotographs.
Sb	present in the colourless glass with slight elevations on red samples, accoutrements of the combatants, especially the degraded scutum on 711, the Retiarius galerus, subligaculum, balteus/cigulum and the Secutor combatant's manica elbow pad. One fleshtone at the Secutor's torso (11078); blue areas, with highest levels on both Secutors' facemasks and shoulder guard; several yellow samples have high levels, especially the Secutores' galea facemasks (aligning with the blues here), balteus/cigulum and scutum front
Hg	below LOD on colourless glass and low elevation on a small number of samples, including brown decorative circle, judge/editor? Hair, blue Secutor shoulder guard and yellow decorative circle and secutor balteus/cigulum. May indicate mixing of cinnabar at these features
Pb	very low traces on the colourless glass. Elevated on a large number of features, especially high on brown Retiarius' subligaculum, galerus, balteus/cigulum and the Secutor's manica below the elbow on 5454 as well as the Secutor scutum with degraded pigment on 711. Also high on the yellow of the Secutor's scutum on 11078, Secutor's (5454) galea facemask and elevated on the yellow decorative circle, Secutor's (11078) balteus/cigulum and in one blue sample of the judge/editor?'s tunic as well as brown of the Secutor's boot degraded pigment (711) and Retiarius' manica and the red inner top of the Secutor's scutum (11078) and Retiarius' galerus

7. Discussion

7.1. General Observations

Detailed comparative studies have confirmed that variability between pXRF and other lab-based techniques, e.g., LA-ICP-MS, for detecting the major elements is sufficiently low as to validate the use of pXRF for this type of analysis [81]. This is especially useful since pXRF provides one of a restrictive repertoire of non-destructive analytical techniques on precious irreplaceable artefacts that cannot be removed from the museum.

Most of the fragments are in a remarkably well-preserved condition with no obvious sign of corrosion or degeneration visible to the naked eye or under a light microscope. Only artefact no. 711 has suffered from corrosion, which is likely the result of post-depositional conditions, possibly relating to alumina and lime which could have penetrated the porous enamelled layer [40]. Aside from elevated K, the elemental composition of these degraded features does not, however, differ markedly from the other painted areas on the glass.

Perhaps surprisingly, the high level of Si present in the base glass is masked on all the painted features where the levels are consistently lower.

The levels of Mn and Sb detected in the colourless base glass are broadly comparable. A slightly elevated Mn might indicate its incorporation as a decolourant or that sodium-rich plant ashes were used as fluxing agents in the creation of the vessel [14,19]. However, the level is only marginally higher than those present on most painted features, aside from some brown samples, which may derive from a natural contaminant in the raw materials used during manufacture [27]. Sb is detected at lower levels on the base glass than on painted features, particularly browns, blues and yellows. Combined, these results confirm that the colourless character of the base glass was likely achieved by using sand with high purity in its manufacture with the potential for low levels of Mn oxide (MnO) added as decolourant agents, as opposed to Sb oxide (Sb₂O₅) [30].

The concentration levels of silica, lime and chlorine can inform colouration processes, but different levels of lead in yellows may be suggestive of workshops in diverse geographic locations, e.g., Egypt or Italy [30]. Certainly, in the absence of Sn together with

very low trace levels of Cr on only a few spots, the use of tin-based opacifiers seen in some vessels from Britain and France (first–second centuries) or chromium colourants [82] is not evidenced. This, along with low levels of Fe, P and Ti present in the base glass, confirms a second–third century date of manufacture through the combined evidence of technology [21] and typology [12].

Other than sharp elevations in the degraded browns on 711 noted above, K is only marginally higher than the base glass in painted areas and consistently maps elevated levels of P and S, confirming this element is associated with the colouring agents present in the enamelling as opposed to the vessel manufacture [18]. It could feasibly derive from sodium-rich plant ash flux in the enamelling glass [14,19] but, given the location of the elevated samples, it could alternatively derive from contact with plant materials in this fragment's post-depositional context. Although this cannot be confirmed purely by pXRF, several parallels with the Lübsow and other beakers suggest enamel-painted features may comprise a soda lime composition in the glass matrix used for the opacifying pigments, as opposed to a lead-based glass [51].

Lead (Pb) and transitional metals (Co and Zn) levels are elevated only on painted features, which may argue against recycled glass [17]. However, we must consider Cu, another transitional metal identified on Late Roman colourless glass of mixed composition from Britain and the Netherlands [15,28], where elevated levels are also present only on enamelled features. Lead could have been deliberately added to serve a variety of purposes, including influencing glass properties, e.g., melting points, expansion and bonding of enamel to the vessel. While it does not directly produce colours, it alters glass structures to change the colours of other metals and creates an environment conducive to the creation of opaque enamel [47]. It can facilitate copper dissolution in the melting phase and the growth of cuprous oxide crystals during cooling, resulting in vibrant reds and oranges [47]. On the Vindolanda vessel the highest levels are recorded in red, brown and yellow areas, indicating Pb is associated with pigments subjected to short episodes of firing at lower than 850 °C, since lead evaporates quickly thereafter [83].

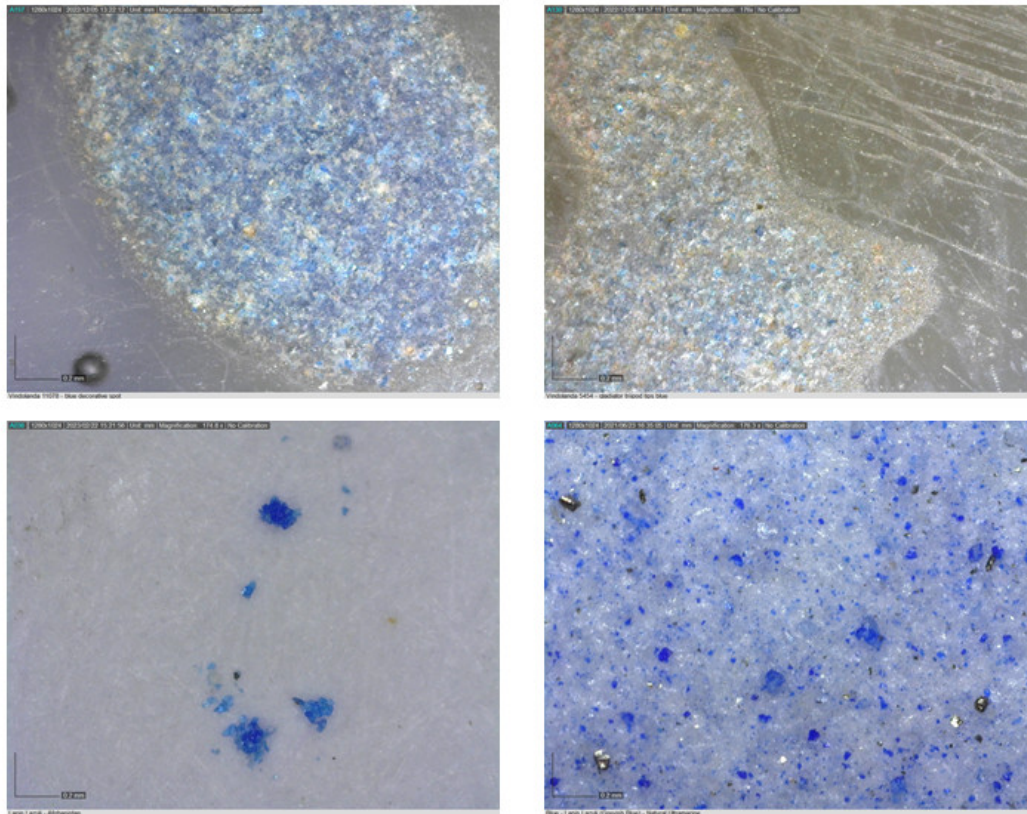
It is helpful to cover in detail the different pigments, and pigment mixtures, identified in various features, and the following addresses these complex compounds by summarising their elemental composition and graphically supporting the presence of the proposed pigments by comparing *in situ* microphotographs of some features with particles of that pigment and how these pigments perform when painted onto paper. The samples derive from Kremer Pigments prepared using authentic traditional techniques and they demonstrate comparable characteristics in colour, texture, shape, crystalline structure and size in all cases.

7.2. Blues

Portable Raman spectroscopy on the Begram beakers identified lapis lazuli on some blue areas and a mixture of lapis lazuli ($\text{Na}_7\text{Al}_6\text{Si}_6\text{O}_{24}\text{S}_3$) (ultramarine) and cobalt minerals in the same matrix of other blue enamelled features [50], a technique also known from enamelled ceramics from Lâjvardina, Iran dating to the thirteenth century [84]. Lapis lazuli has also been identified using Micro-Raman in blue features painted onto the Lübsow beakers thought to be the earliest known examples of natural lazurite used as an enamel opacifier [51]. That unanticipated discovery stimulates questions on what other pigments may have been used on enamelling, subject to a basic requirement of their ability to tolerate high firing temperatures up to c. 1000 °C [49]. Lapis lazuli was also used for blue enamelling on a glass 'circus cup' from a grave at Ellekilde, Denmark, where it was identified in a copper-doped turquoise glass matrix and cobalt-doped blue glass matrix [40].

The Geochem2 mode of the Olympus Vanta does not detect Na and levels of Al, Si and S are not elevated in most of the blue samples, although high Ca and Fe are and microphotographs on some blue features, e.g., a decorative dot and the *Secutores'* fascinas and weaponry, conform with the character of lapis lazuli (Figure 10) and certainly confirm the presence of pigment particles. The results show a slight elevation in K consistent with

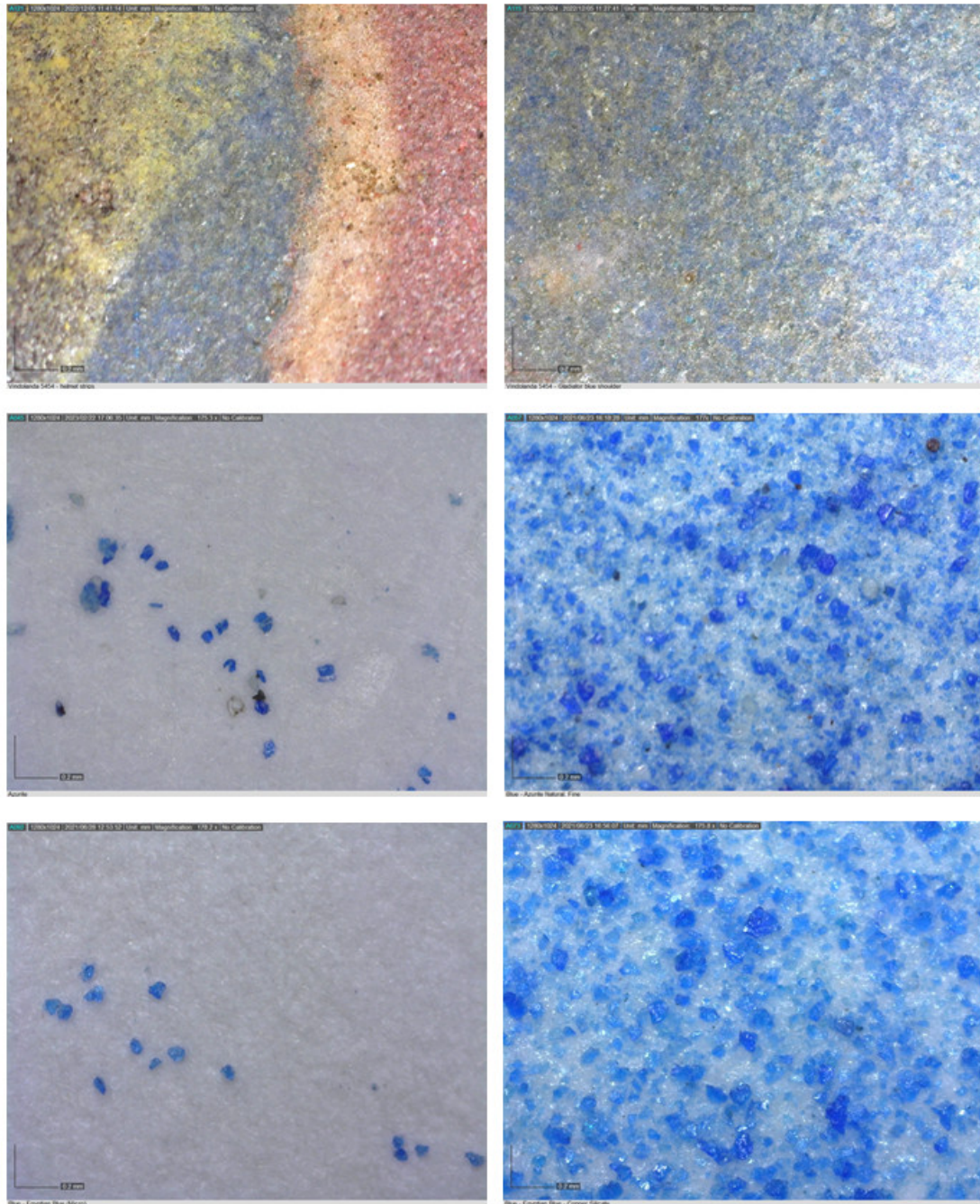
lapis lazuli [85], but it is not significantly higher than other painted features except some degraded brown samples where K is significantly increased (see above). Traces of Ca and Fe have also been found to correspond with impurities naturally present in lapis lazuli [86], so its presence here is feasible.



Microphotograph Scale
0.2mm

Figure 10. Lapis lazuli pigment in the matrix of (top): a blue decorative spot (left) *Retiarius'* fascia (right); and (bottom): microscopic sample of lapis lazuli (left) and pigment painted on paper (right), images taken with Dinolite microscope @ 175× magnification.

It is possible that, like the Ellekilde cup, lapis lazuli pigments were mixed with cobalt or in a copper or cobalt-doped blue glass matrices [40]. However, given the high level of Cu elevation predominantly on blue features (but see below), the presence of another pigment, azurite—a basic copper (II)-carbonate ($\text{Cu}_3(\text{CO}_3)_2(\text{OH})_2$), in the facemask, shoulder guard of the *Secutor* on artefact no. 5454 and *fascina* of the *Retiarius* is also a possibility (Figure 11). The consistently very highly elevated readings of Cu and low levels of Pb [87] alongside Fe, Ca and K reported above, combined with the characteristics recorded in microphotographs, confirm that azurite produces a darker, more intense and less refractive character of blue to lapis lazuli alone. Some refractive properties remain in these samples which aligns with the pXRF results, making it possible azurite was mixed with lapis lazuli here to depict more intense and deeper blue on metalwork associated with protective gear.



Microphotograph Scale
0.2mm

Figure 11. Additional blue pigment applied to the *Secutores'* galea (top left) and shoulder pad (top right); microscopic sample of azurite (centre left) and pigment painted on paper (centre right); microscopic sample of Egyptian blue (bottom left) and pigment painted on paper (bottom right), image taken with Dinolite microscope @ 175× magnification.

Another possibility is Egyptian blue, an artificial copper calcium silicate ($\text{CaCuSi}_4\text{O}_{10}$) which could explain the elevated Ca and Cu, if not the Si which is masked by the base glass in all painted features, though it is very slightly higher in these areas than other features. Egyptian blue depicting metal military protective equipment and weaponry is evident on sculpted reliefs, such as on the Nicomedia relief [88], and a planned follow-up

programme of multi-spectral imaging will clarify this using Visible-Induced Luminescence Imaging (VIL) techniques. So, while elevated levels of Cu reduce the probability for these blue pigments to two candidates, Egyptian blue is the more likely candidate than azurite given the associated elevation of Ca restricted to blue samples across the vessel. See Figure 12 for example pXRF spectra from blue samples.

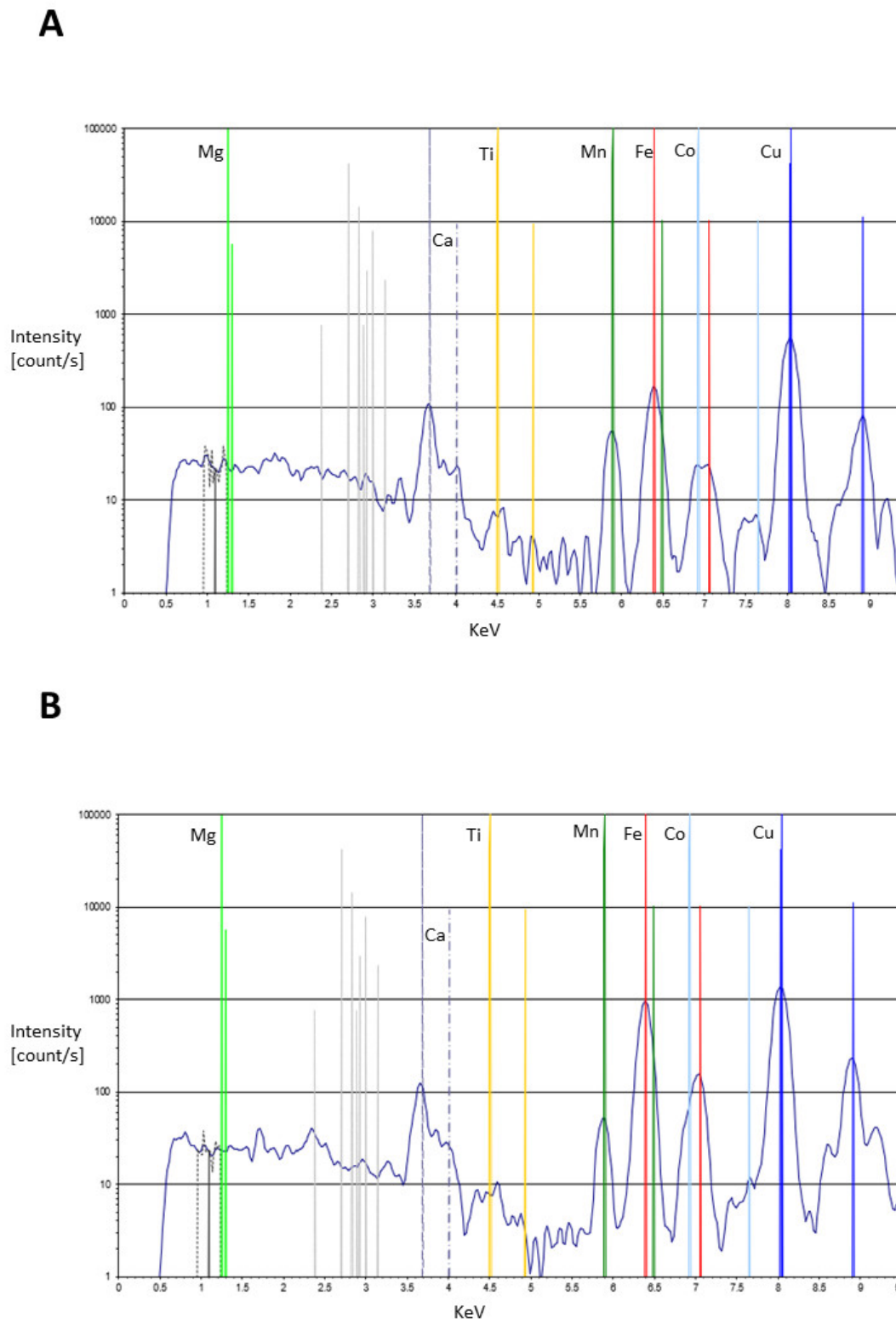


Figure 12. Examples of Blue spectra—(A) Sample No. n22 (blue—*Secutor gladius* blade); (B) Sample No. 15 (blue mix—*Secutor galea* facemask).

Certainly, this blue differs in colour and character to the other samples above, with a viscous matrix that could result from Egyptian blue's manufacturing technique of heating calcium and copper compounds with silica and natron and could, therefore, lend itself perfectly to high firing temperatures and adhering to a glass vessel. A greenish derivative of Egyptian blue was used by glassmakers and potters since Egyptian times and in later (eighth C) Tang porcelains [49], providing a precedent for its use in this context. Its detection here as an ingredient for Roman glass enamelling constitutes a ground-breaking discovery.

7.3. Reds and Browns

Fe is highly concentrated in almost all painted features, particularly highest in reds and browns as well as flesh tones, some blue areas (decorative circle and the *manica*, face-mask and shoulder guard of the *Secutores*) and yellow on the *Secutores'* facemasks. This suggests iron oxide hematite, red ochre (Fe_2O_3), probably mixed into a soda glass binder for these areas, in contrast to low Fe levels on the background colourless glass which confirms its manufacture from sand with high-purity and low iron [16].

In these features there is evidence for much elemental diversity, indicating a complex mixing of different materials, including hematite, lead antimony, possibly realgar/orpiment (see below) and traces of cinnabar in the reds and browns as well as possibly green earth in the browns given the detection of highly elevated Al (see Table 5 for full details) and a visible greenish hue to some brownish features (Figure 13). Occasional very bright red spots in the red matrices certainly hint at trace amounts of cinnabar and this is supported by traces of Hg in the pXRF results (see Figure 9), although the levels are so low as to not be visibly detectable in the scale of the spectra; some examples are provided in Figure 14.

Table 5. Palette of pigments.

Coloured Features	Elements Detected by pXRF	Pigment/s	Compound/s
Blue (1)	Al, Ca, Fe, K (trace)	Lapis lazuli	$\text{Na}_7\text{Al}_6\text{Si}_6\text{O}_{24}\text{S}_3$
Blue (2)	Ca, Fe, Cu, Co	Azurite	$\text{Cu}_3(\text{CO}_3)_2(\text{OH})_2$
Blue (3)	Ca, Fe, Cu, Si (trace)	Egyptian Blue	$\text{CaCuSi}_4\text{O}_{10}$
Brown	Mg, Al, Fe, Cu, As, Sb, Pb, Hg (trace)	Iron oxide (hematite);	Fe_2O_3
		Green Earth?	$\text{K}[(\text{Al}, \text{Fe}^{\text{III}}), (\text{Fe}^{\text{II}}, \text{Mg})](\text{AlSi}_3, \text{Si}_4)\text{O}_{10}(\text{OH})_2$
		Azurite?;	$\text{Cu}_3(\text{CO}_3)_2(\text{OH})_2$
		Lead antimonate;	$\text{Pb}_2\text{Sb}_2\text{O}_7$
		Realgar;	As_2S_3
Cinnabar (trace)	HgS		
Cream	Fe, Cu, Pb	Iron oxide (hematite);	Fe_2O_3
		Lead antimonate;	$\text{Pb}_2\text{Sb}_2\text{O}_7$
		Azurite?	$\text{Cu}_3(\text{CO}_3)_2(\text{OH})_2$
Red	Fe, Cu, As, Sb, Pb, Hg (trace)	Iron oxide (hematite);	Fe_2O_3
		Minium?;	Pb_3O_4
		Azurite?;	$\text{Cu}_3(\text{CO}_3)_2(\text{OH})_2$
		Lead antimonate;	$\text{Pb}_2\text{Sb}_2\text{O}_7$
		Realgar;	As_2S_3
Cinnabar (trace)	HgS		
Flesh tone	Mg, Al, Ca, Fe, Ti, Cu, As, Sb, Pb	Iron oxide (hematite);	Fe_2O_3
		Lead antimonate;	$\text{Pb}_2\text{Sb}_2\text{O}_7$
		Green earth;	$\text{K}[(\text{Al}, \text{Fe}^{\text{III}}), (\text{Fe}^{\text{II}}, \text{Mg})](\text{AlSi}_3, \text{Si}_4)\text{O}_{10}(\text{OH})_2$
		Orpiment;	As_2S_3
Azurite?	$\text{Cu}_3(\text{CO}_3)_2(\text{OH})_2$		
Yellow	Al, Ti, Fe, Cu, As, Sb, Pb, Hg (trace)	Iron oxide (hematite or goethite)	Fe_2O_3 , or $\alpha\text{-FeOOH}$
		Lead antimonate;	$\text{Pb}_2\text{Sb}_2\text{O}_7$
		Orpiment;	As_2S_3
		Green earth;	$\text{K}[(\text{Al}, \text{Fe}^{\text{III}}), (\text{Fe}^{\text{II}}, \text{Mg})](\text{AlSi}_3, \text{Si}_4)\text{O}_{10}(\text{OH})_2$
		Azurite?	$\text{Cu}_3(\text{CO}_3)_2(\text{OH})_2$

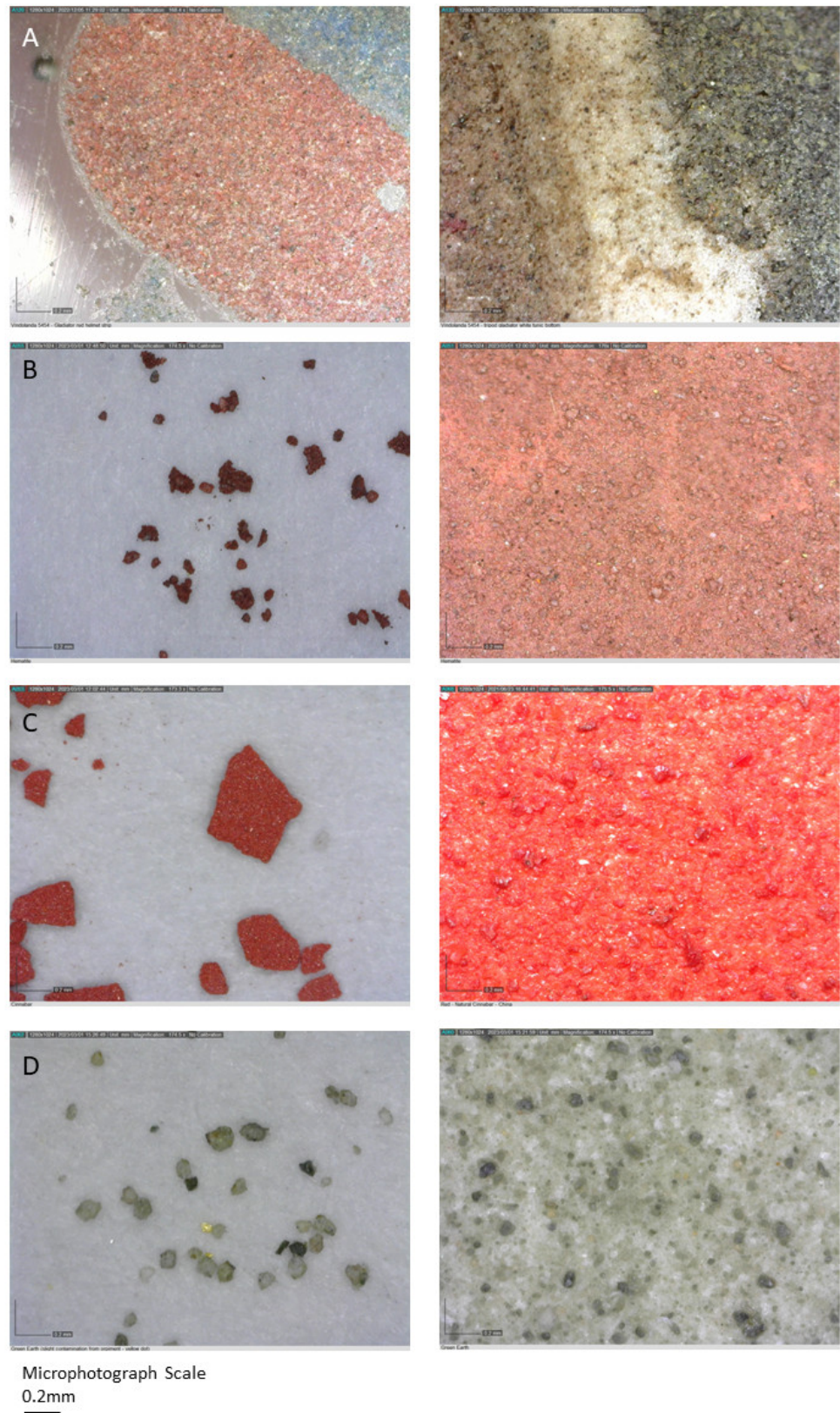


Figure 13. (A)—Red on Secutor's gallea (left); brown on *Retiarius' subligaculum* (right); (B)—microscopic sample of hematite (left) and pigment painted on paper (right); (C)—microscopic sample of cinnabar (left) and pigment painted on paper (right); (D)—microscopic sample of green earth (left) and painted on paper (right), images taken with Dinolite microscope @ 175× magnification.

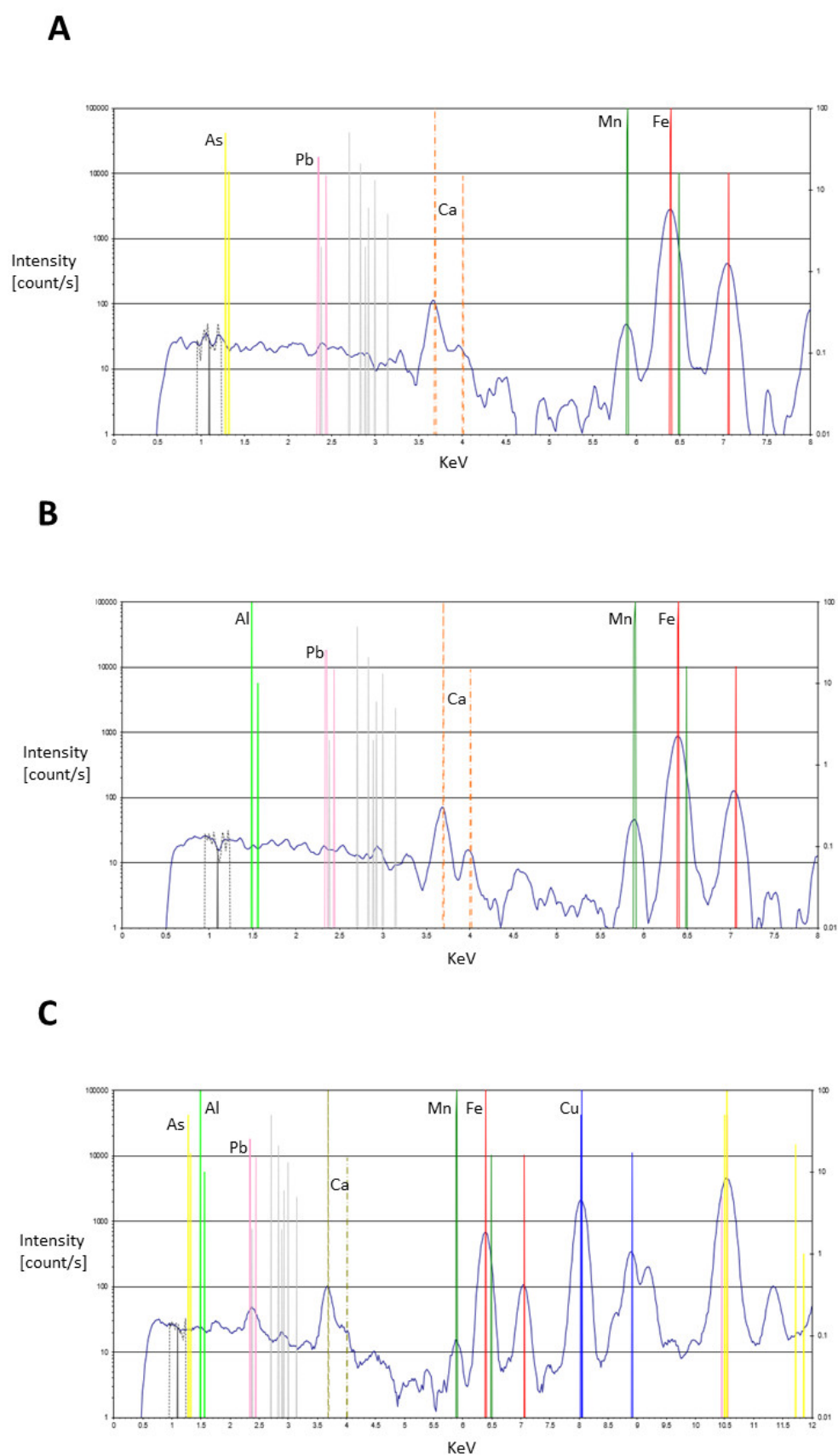


Figure 14. Examples of Red and Brown spectra—(A) Sample No. 27 (red—decorative band under *Retiarius*); (B) Sample No. n2 (brown—judge/editor? eye); (C) Sample No. 9 (brown mixture—*Retiarius balteus/cigulum*).

The presence of cinnabar as an enamel colourant is another ground-breaking discovery.

This practice of mixing and layering different enamels to achieve desired colours is confirmed for the Ellekilde [40] and Lübsow vessels [51]. Although it cannot be confirmed with certainty, given the high Pb content, minium (Pb_3O_4) could also be in the mix, in line with a reference made in a study of various Roman enamelled glass [50], but that comment is not supported or discussed in the published analytical results. Certainly, this pigment is prepared by heating at very high temperatures so it is not unreasonable to suggest it could tolerate the high temperatures of the glassmaker's kiln and provide the lead required to colour enamel glass [47].

The intensive Raman mapping of blue enamelling on Roman glass has further identified a complex, and unexpected, mix of hematite, lazurite, diopside and cobalt spinel. While the authors discount the presence of hematite as "hardly added on purpose" [50] (p. 4350) and attribute it to a by-product of roasting the pyrite naturally present in lapis lazuli, it is most interesting to note its presence here along with the mix of other pigments. The use of copper-doped glass matrix for the enamelling on these features is possible, but unlikely (see above). More likely, mixing or layering or contamination from azurite/Egyptian blue could explain the elevated Cu in some samples close to blue areas or layered features, such as the highest two readings deriving from areas relating to the *Retiarius* visibly painted in layers. This proposal is supported by the layering and mixing of different particles evident in several microphotographs, perhaps most notably the judge/editor? Tunic and face and *Secutores'* facemasks (Figure 9). It is alternatively possible that the high Cu derives from the copper or cuprous oxide used in some Roman enamelling (see Table 1), but the levels are not sufficiently elevated to support that in comparison to the high levels identified in blue features and the excessively high levels of Fe in reds and browns point definitively to an iron oxide.

This aligns with the Lübsow analysis which also detected hematite in red enamelled areas, confirming the mixing of iron oxide with a soda glass binder which differs from the more common technique of colouring opaque red glass and enamel with precipitated copper compounds [51]. There, reds with elevated iron oxide (20%) combined with low lead and high silica indicate that soda-lime-silica glass pigment binder was used, as with the blues, made with transparent blue glass opacified with white antimony compound, probably calcium antimonate as with the Ellekilde cup, where hematite was also detected [40].

7.4. Yellows

Yellows in mosaic glass vessels dating from the first–third century contain lower levels of iron oxide and elevated Pb correlating with higher Sb [30]. This appears to broadly correlate with the yellow enamels on the Vindolanda yellows, suggesting a lead-rich material as with the yellow enamels on the Lübsow and Ellekilde vessels [40,51]. Micro-Raman on the latter two confirmed lead antimonate ($Pb_2Sb_2O_7$) and the pXRF results combined with microphotographs (Figure 15) from the Vindolanda vessel showing the typical porous structure and heterogeneous character associated with lead antimonate correlate with this, confirming its presence in the yellow and mixed into the red and brown features where hematite is also identified. Both hematite and lead antimonate have low melting temperatures, making them excellent materials for enamelling.

Again, the mixing or layering of pigments is clearly visible in these areas from the microphotographs of, for example, the *Secutor's* boot and *galea*. The elevated levels of Al, Ti, Fe, Cu and As suggest the presence of iron oxide (hematite or goethite), possibly some green earth and a copper-based pigment, likely azurite or Egyptian blue (blue flecks visible in the matrix of yellow features, and see above) as well as an additional yellow pigment—orpiment (As_2S_3)—where pigment particles are visible in the microphotographs of several yellow features.

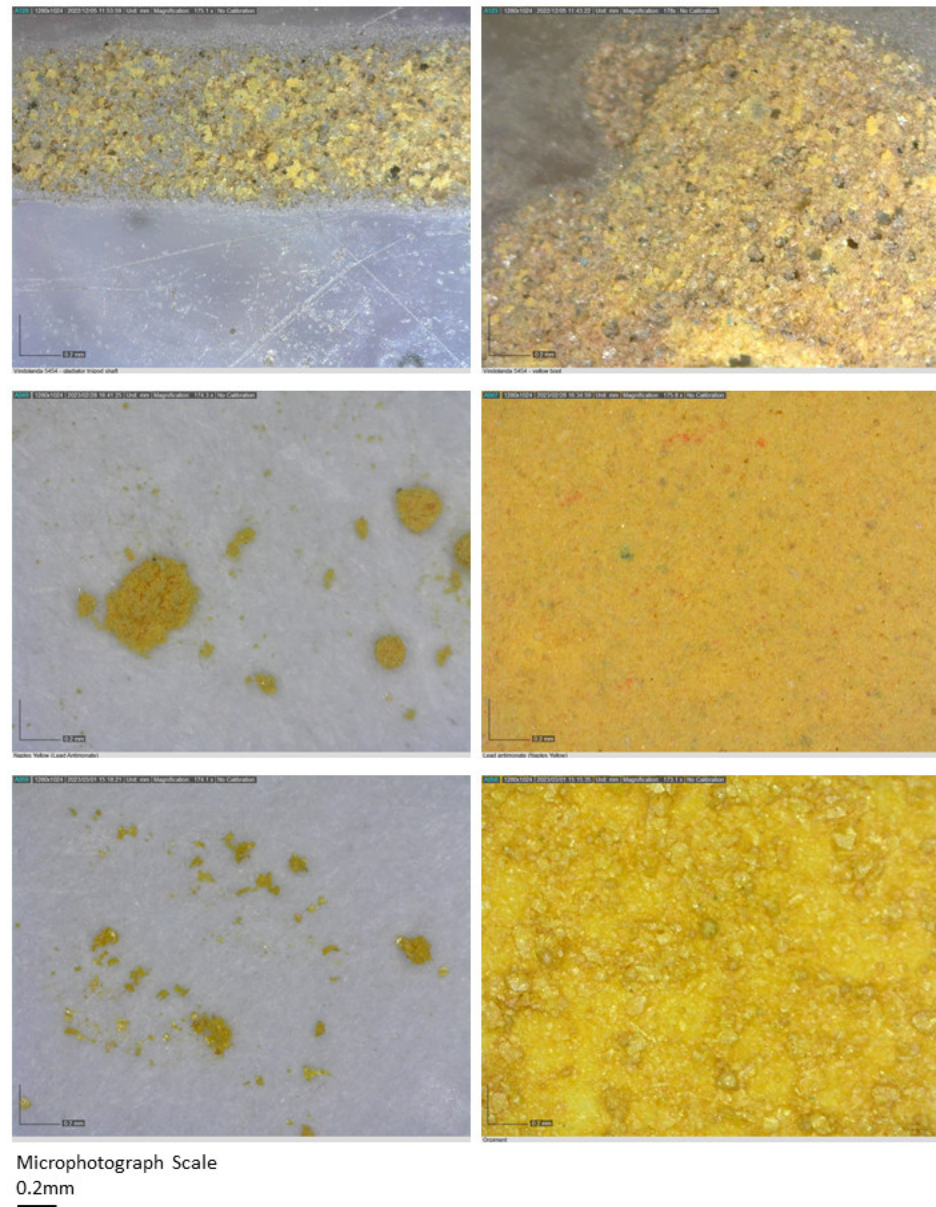


Figure 15. Yellow features on Vindolanda vessel (**top**) *Retiarius' fascina* shaft (**left**) and *Secutor's* boot (**right**); (**centre**) microscopic sample of lead antimonate (**left**) and pigment painted on paper (**right**); (**bottom**) microscopic sample of orpiment (**left**) and pigment painted on paper (**right**), images taken with Dinolite microscope @ 175× magnification.

Orpiment is a toxic arsenic sulfide mineral that is the product of hydrothermal veins or volcanic sublimation commonly used as a pigment since Egyptian times to represent gold in artworks and known to the Romans as Auripigmentum [2] (33.22). Like Egyptian blue (see above), orpiment has not previously been considered a constituent of Roman enamelling recipes; however, its presence is confirmed by the direct correlation between elevated As and S, especially in yellow and brown features. This is graphically illustrated in Figure 16A, demonstrating a clear correlation between the As peak at 1.28–1.32 KeV confirming the presence of arsenic as opposed to interference from Pb peaks, which is a known effect of these two elements with the pXRF technique. Further verification is provided by the detection of arsenic in Byzantine enamelled bracelets proposed to derive from orpiment [89], so it is reasonable to conclude its use for enamelling stretches back to the Roman period. Again, like Egyptian blue, orpiment derives from high heat sources so

its properties are conducive to being exposed to the high firing temperatures of the glass-maker's kiln.

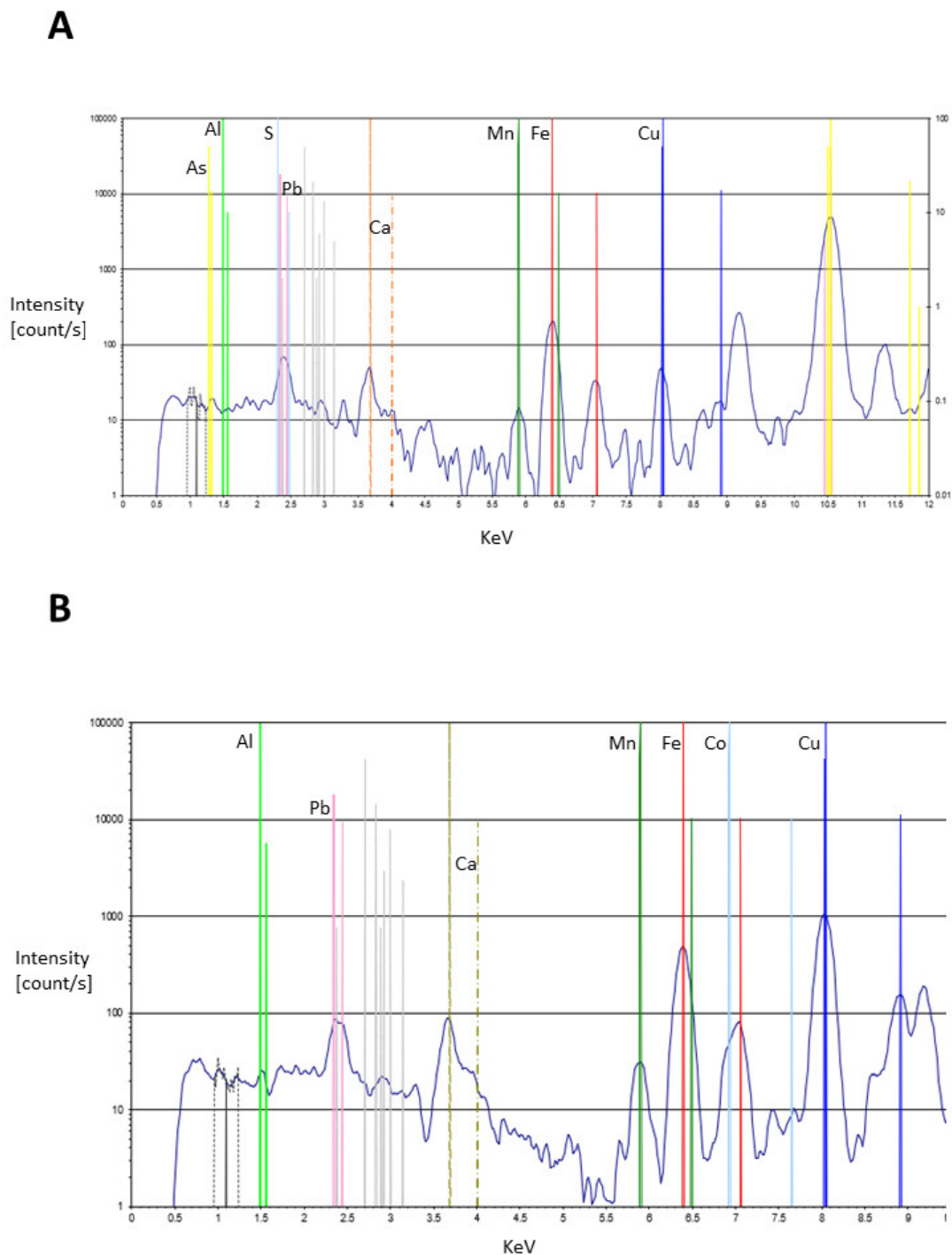


Figure 16. Examples of Yellow spectra—(A) Sample No. n19 (yellow-cream—*Secutor scutum* front); (B) Sample No. 16 (yellow mixture—*Secutor galea* facemask).

Its confirmed presence here constitutes yet another ground-breaking discovery.

7.5. Creams and Fleshtones

Calcium antimonate (CaSb_2O_6) as a white opacifier was detected on enamelled features on the Ellekilde [40] and Lübsow vessels, correlating with Roman enamelling on

metals as well as beads and tesserae [51]. Raman on other examples of Roman glass also confirms white enamels created using cassiterite and calcium phosphate [50]. Although Ca and Sb levels are not elevated in these features, the cream and fleshtone surfaces with dark dispersed inclusions on our Vindolanda vessel are visibly more opaque and heterogeneous in character than all other colours. They find parallels with the calcium antimonate used, for example, on funerary artwork from Paestum, Italy where it was mixed with ochres and hematite similar to ceramic painters influenced by glassmakers during third–sixth century BCE [90]. That said, high Fe, Cu and Pb are detected in both cream and fleshtones (see Figure 9), with elevated Mg, Al and K in the fleshtones along with Ti, As, Sb and Pb. This suggests the mixing of iron oxide (hematite), and lead antimonate in both colours, with the addition of green earth, orpiment/realgar and possibly azurite or Egyptian blue to create fleshtones.

The combined results confirm demonstrable quantitative differences between the various coloured features on the Vindolanda glass vessel that permit the identification of the pigments present, summarised in Table 5 where the complex compounds of pigments are indicated. Although it has not been possible to deploy X-Ray Diffraction or Raman Spectroscopy to fully extrapolate the compounds present, visual inspection combined with digital microphotography make clear that some features have been applied in layers, for example, the yellow painted over blue on the *Secutores'* galea and *Retiarius'* *balteus/cigulum* onto the brown *subligaculum*. Microscopic evidence for pigment mixing further complicates matters, which is particularly evident in the tunic of the judge/editor? as well as the yellow and brown features, such as close to the *Retiarius'* *balteus/cigulum* where the particles of other colours (red and blue) are clearly visible in the matrices. This practice introduces additional layers of complexity into the analysis since the pXRF provides the summative results of elements present in samples, irrespective of their stratigraphy. However, the elements associated with particular pigments are clearly evident in specific contexts which align with visible evidence of mixing/layering. This provides confidence in the recipes suggested for some of the features to produce desired hues. The pigments listed in Table 5, therefore, provide a summary of the pigments that have been identified in *some* features to create different hues, so they are not *all* present in the recipe for every coloured context.

8. Conclusions

The remarkably well preserved Vindolanda vessel is not a mass-produced moulded glass souvenir depicting gladiatorial games of the type found across Rome's western provinces. This is a unique and individually crafted artefact that is unparalleled in the quality of the colourless glass used in its creation and the enamel-painted artwork articulated at the hand of a highly skilled artisan. The use of antimony-based opacifiers in glass production stretches back to 1500 BCE in Egypt and the Near East, but we are not seeing this in the Vindolanda vessel and there is no correlation between Ca and Sb to indicate the presence of calcium-based antimonate decolourants. Rather, the correlation between Pb and Sb only on enamelled areas confirm that lead-based antimonates are restricted to enamelling products deriving from a different glass used in the artwork, perhaps to make the colours more vibrant and translucent. Occasional black spots visible under microscopy in the lighter coloured features support this. This, together with low levels of Fe, P and Ti and the absence of Mn and Sb and Fe decolourants in the base glass combine to verify second–third century date of manufacture [21] from sand of high purity, possibly from a workshop in the Eastern Mediterranean. Negligible levels of impurities from Ba, Cr, Cl, Ti and Pb [64] further confirm the purity of the base glass.

This pushes its manufacture definitively beyond established thinking on the chronology of some enamelled glassware, such as the cups from Locarno and Masada. However, the quality and composition of the Vindolanda base glass, combined with the application technique and articulation of artwork, make a later date plausible. This is supported by the proposal that the Masada vessels may be the earliest examples containing gladiatorial

combat scenes and their disturbed contexts of discovery could be attributed to any of the occupational levels from between the first and seventh centuries [46]. Previous reliance upon only a few excavated examples of Isings Form 12 for dating the Masada cups [91] lends further credence to a later date suggested for a Roman enamelled glass fragment than it was previously assigned [92] and certainly prompts the reconsideration of this vessel class chronology.

Indeed, elevated transitional metals, including Pb, Co, Zn [17] and Cu on the Vindolanda vessel, suggest a later manufacturing date for the enamelling glass which differs significantly from the base vessel and may have been enamelled in a different workshop, possibly even the western provinces, later than the first century [15,28]. If further validation is needed, the use of hematite as an opacifier is rare, largely due to iron oxides dissolving in glass melts, and more commonly attributed to later Islamic and Venetian traditions [51] so their use in a cold-mixed soda glass enamel is highly unlikely to date from the first century when the technique was in its infancy. Leading on from that, the refinement of technologies and the innovation of specialist artisans favours experimentation with different, widely available, pigments as enamelling skills developed, and this aligns with the typology of this Ising 85B vessel which dates it to the late second to first half of the third century [69].

We can say something about the manufacturing process for the enamelling insofar as the survival of iron oxide confirms a very short firing period for the enamelling phase, otherwise these would have dissolved in the glass melts [51]. The firing temperature for this phase cannot have exceeded 720 °C since the sulphur contents of lazurite cannot survive beyond that [92,93] and temperatures between 600–800 °C are generally used to achieve the desired hues and texture of enamel painting [66]. The evidence for lead evaporating beyond 850 °C further validates this.

The pXRF results confirm complex recipes of mixed pigments for enamelling, a proposal that cannot be disproved given the absence of experimental work with pigments on Roman glass to ascertain their behaviour during episodic firing at different temperatures. This is a situation that will soon be addressed through experimentation with colleagues specialising in this field with the necessary glassworking expertise to monitor and control the variable and complex processes involved. That said, the results for some pigments, including lapis lazuli, hematite and lead antimonate find parallels in other Roman enamelled glassware and there is reason to suggest other pigments could tolerate quick firing that experimental work found was sufficient to affix 'harder' colours like reds and yellows, with a grainy surface effect [36]. However, that experimental work appears to have used modern glass compositions since it reports only on crushing some yellow glass and not on whether enamels were made from first principles or using pigments.

Lapis lazuli and hematite are known to have properties conducive to the high temperatures of the glassworker's kiln, and the mixing of, for example, lapis lazuli and lead antimonate to create green has been identified in some cases through Raman spectroscopy [50]. However, other pigments have not been studied to determine their tolerance to similar conditions or how mixtures are created beyond the basic known component colourants. Therefore, the identification of Egyptian blue, orpiment and cinnabar and possibly minium and green earth here in complex recipes to create a vibrant palette is an exciting and revolutionary development that breaks new ground in this field. Certainly, the presence of Egyptian blue and orpiment confirmed from the pXRF results and microscopy verifies that they possess the necessary properties to tolerate enamelling manufacturing techniques.

The planned programme of experimental work in collaboration with heritage glass specialists will systematically explore this issue using authentic pigments.

Supplementary Materials: The following supporting information can be downloaded at: www.mdpi.com/xxx/s1, Table S1: Concentrations of main all of the main elements identified by pXRF.

Funding: Grant funding was most gratefully received from Historic Environment Scotland (Grant Number HEAP2470491033), the University of Glasgow's Lord Kelvin Adam Smith Leadership Fellowship.

Data Availability Statement: The datasets used and analysed during the current study are available from the author on reasonable request.

Acknowledgments: Sincere thanks are due to several individuals, particularly Barbara Birley and the Vindolanda Trust for providing access to the Vindolanda vessel; Denise Allen, David Hill and Mark Taylor for sharing insightful comments on the technological processes involved in Roman glassmaking and enamelling, as well as their tremendously helpful comments on the text and graphics which have greatly strengthened the paper; Carole Raddato for permission to use images and Margaret Smith for comments and suggestions for the refinement of the arguments contained herein. Thanks are also due to Bernie Hammersley for insights into combat methods and stances which informed the discussion on iconography. Any errors or points of controversy rest entirely with the author.

Conflicts of Interest: The author declares no conflicts of interest.

References

1. The Glassmakers: 3500 years of glass and counting... Available online: <http://www.theglassmakers.co.uk/> (accessed on 3 April 2023).
2. Elder, P.T. *Naturalis Historia*; Rackham, H., Translator; Harvard University Press: Cambridge, UK, 1938. https://doi.org/10.4159/DLCL.pliny_elder-natural_history.1938.
3. Tatton-Brown, V.; Andrews, C. Before the Invention of Glassblowing. In *Glass, 5,000 Years*; Tait, H., Ed.; H.N. Abrams: New York, NY, USA, 1991; pp. 21–61.
4. Cool, H.E.M. The Vessel Glass. In *Silchester Insula IX: The Claudio-Neronian Occupation of the Iron Age Oppidum: The Early Roman Occupation at Silchester Insula IX, Britannia Monograph Series 33*; Fulford, M., Clarke, A., Durham, E., Pankhurst, N., Eds.; Society for the Promotion of Roman Studies: London, UK, 2020; pp. 302–319.
5. Harden, D.B.; Kemper, H.; Painter, K.; Whitehouse, D. (Eds.). *Glass of the Caesars*; Olivetti: Milan, Italy, 1987.
6. Barag, D.P. Towards a Chronology of Syro-Palestinian Glass. In *Annales du 8e Congrès International, d'Etude Historique du Verre: Londres-Liverpool, 18–25 September 1979*; Association Internationale pur L'Histoire du Verre: Liège, Belgium, 1981; pp. 73–81.
7. Cool, H.E.M. *The Small Finds and Vessel Glass from Insula VI. 1 Pompeii: Excavations 1995–2006*; Archaeopress: Oxford, UK, 2016.
8. Hill, D. (The Glassmakers, Andover, Hampshire, UK); Taylor, M. (The Glassmakers, Andover, Hampshire, UK) Personal communication, 2023.
9. Pitzer, A.P.S. Exploring Value through Roman Glass from Karanis, Egypt. PhD Thesis, University of California, Los Angeles, CA, USA, 2015. Available online: <https://escholarship.org/uc/item/9nt4r3vr> (accessed on 12 January 2023).
10. Cottam, S.E. Developments in Roman Glass Vessels in Italy, France, Britain and the Lower Rhineland c. AD40–AD110. PhD Thesis, King's College, London, UK, 2019, Unpublished. Available online: https://kclpure.kcl.ac.uk/portal/files/116534678/2019_Cottam_Sally_098227_thesis.pdf (accessed on 12 January 2023).
11. Cassibry, K. Spectacular Translucence: The Games in Glass. *Theor. Rom. Archaeol. J.* **2018**, *1*, 5. <https://doi.org/10.16995/traj.359>.
12. Price, A.J.; Cottam, S.E. *Romano-British Glass Vessels: A Handbook, Practical Handbook in Archaeology 14*; Council for British Archaeology: York, UK, 1998.
13. Baxter, M.J.; Cool, H.E.M.; Heyworth, M.P.; Jackson, C.M. Further studies in the compositional variety of colourless Romano-British vessel glass. *Archaeometry* **2005**, *37*, 47–68.
14. Henderson, J. *Ancient Glass*; Cambridge University Press: Cambridge, UK, 2013.
15. Huisman, D.J.T.; Groot, D.E.; Pols, S.; Van Os, B.J.H.; Degryse, P. Compositional Variation in Roman Colourless Glass Objects from the Bocholtz Burial (The Netherlands). *Archaeometry* **2009**, *51*, 413–439.
16. Jackson, C.M. Making Colourless Glass in the Roman Period. *Archaeometry* **2005**, *47*, 763–780.
17. Degryse, P. Isotopes-Ratio Techniques in Glass Studies. In *Modern Methods of Analysing Archaeological and Historical Glass, I*; Janssens, K.A., Ed.; John Wiley & Sons, Ltd.: Chichester, UK, 2013; pp. 235–245.
18. Tantrakarn, K.; Kato, N.; Hokura, A.; Nakai, I.; Fujii, Y.; Gluščević, S. Archaeological analysis of Roman glass excavated from Zadar, Croatia by newly developed portable XRF spectrometer for glass. *X Ray Spectrom.* **2009**, *38*, 121–127.
19. Foy, D.; Picon, M.; Vichy, M.; Thirion-Merle, V. Caractérisation des verres de la fin de l'Antiquité en Méditerranée occidentale: l'émergence de nouveaux courants commerciaux. In *Echanges et Commerce du verre dans le Monde Antique, Proceedings of the Acts of the AFAV Conference, Aix-en-Provence and Marseilles, France, 7–9 June 2001*; Foy, D., Nenna, M.D., Eds.; Editions Mergoïl: Dremil-Lafage, France, 2003; pp. 41–85.

20. Price, J. Glass-working and glassworkers in cities and towns. In *Roman Working Lives and Urban Living*; MacMahon, A., Price, J., Eds.; Oxbow Books: Oxford, UK, 2005; pp. 167–190.
21. Jackson, C.; Foster, H. Provenance Studies and Roman Glass. In *Glass of the Roman World*; Bayley, J., Freestone, I.C., Jackson, C.P., Eds.; Oxbow Books Ltd.: Oxford, UK, 2015; pp. 44–56.
22. Freestone, I.C.; Bimson, M.; Buckton, D. Compositional categories of Byzantine glass tesserae. In *Annales du 11e Congrès de l'Association Internationale pour l'Histoire du Verre, Bâle, 29 Août–3 Septembre 1988*; AIHV: Amsterdam, The Netherlands, 1990; pp. 271–281.
23. Turner, W.E.S.; Rooksby, H.P. A study of opalising agents in ancient opal glasses throughout three thousand four hundred years. *Glastech. Ber.* **1959**, *VII*, 17–28.
24. Henderson, J.; Warren, S.E. Analysis of prehistoric lead glass. In Proceedings of the 22nd Symposium on Archaeometry, Bradford, UK, 30 March–3 April 1982; Aspinall, A., Warren, S.E., Eds.; University of Bradford: Bradford, UK, 1983, pp. 83–94.
25. Tite, M.; Pradell, T.; Shortland, A. Discovery, Production and use of tin-based opacifiers in glasses, enamels and glazes from the late Iron Age onwards: A reassessment. *Archaeometry* **2006**, *50*, 67–84.
26. Henderson, J. Scientific Analysis of ancient glass. In *Scientific Analysis in Archaeology*; Henderson, J., Ed.; Oxford University Committee for Archaeology Monograph No. 19: Oxford, UK, 1989, pp. 30–60.
27. Turner, W.E.S. Studies in ancient glasses and glassmaking processes, part III: The chronology of the glass-making constituents. *J. Glass Technol.* **1956**, *40*, 39–52.
28. Paynter, S. Analyses of Colourless Roman Glass from Binchester, County Durham. *J. Archaeol. Sci.* **2006**, *33*, 1037–57.
29. Foster, H.E.; Jackson, C.M. The Composition of Late Romano-British Colourless Vessel Glass: Glass Production and Consumption. *J. Archaeol. Sci.* **2010**, *37*, 3068–3080.
30. Freestone, I.C.; Stapleton, C.P. Composition, Technology and Production of Coloured Glasses from Roman Mosaic Vessels. In *Glass of the Roman World*; Bayley, J., Freestone, I.C., Jackson, C.P., Eds.; Oxbow Books Ltd.: Oxford, UK, 2015; pp. 61–76.
31. Jackson, C.M.; Paynter, S. A Great Big Melting Pot: Exploring patterns of glass supply, consumption and recycling in Roman Coppergate, York. *Archaeometry* **2016**, *58*, 68–95.
32. Dalton, O.M. *Byzantine Art and Archaeology*; Dover Publications: New York, NY, USA, 1961.
33. Pierides, A. *Jewellery in the Cyprus Museum*; Department of Antiquities: Nicosia, Cyprus, 1971.
34. Cooper, E. *Ten Thousand Years of Pottery*, 4th ed.; University of Pennsylvania Press; Philadelphia, PA, USA, 2000.
35. Van der Linden, V.; Meedsom, E.; Devos, A.; Dooren, R.V.; Nieuwdorp, H.; Janssen El Balance, S.; Vekemans, B.; Vincze, L.; Janssen, K. PXRF, μ -XRF, Vacuum μ -XRF, and EPMA Analysis of Email *Champlevé* Objects Present in Belgian Museums. *Microsc. Microanal.* **2011**, *17*, 675–685.
36. Gudenrath, W. Enameled Glass Vessels, 1425 B.C.E.-1800: The Decorating Process. *J. Glass Stud.* **2006**, *48*, 23–70.
37. Taylor, M. (Owner, The Glassmakers, Andover, Hampshire, UK). Personal communication, 2023.
38. Norling-Christensen, H. Romerske glaskar i Danmark. *Nationmuseets Arb.* **1953**, 81–90.
39. Ekholm, G. Westeuropäische Gläser in Skandinavien während der späten Kaiser—Und der frühen Merowingerzeit. *Acta Archaeol.* **1958**, *29*, 21–50.
40. Greiff, S.; Hartman, S. Scientific studies on fragments of enamelled glass from a 'circus cup'. In *Aarbøger for Nordisk Oldkyndighed og Historie*; J.H. Lyng & Son: Copenhagen, Denmark, 2009; pp. 121–132.
41. Słowińska, D.; Kejtrowska, K.; Hansen, U.L. A Roman painted glass beaker from Przeworsk culture cemetery at Zaborów, Western Mazowsze. *Wiadomości Archeol.* **2008**, *60*, 125–160.
42. Fehr, H.; Welker, E. Reiche römische Brandbestattung mit bemaltem Glasbecher aus Bassenheim Kreis Mayen-Koblenz. *Archäologisches Korresp.* **1986**, *16*, 193–198.
43. Allen, D. (Independent researcher, Devon, UK). Personal communication, 2023.
44. Coarelli, F. The Painted Cups of Begram and the Ambrosian Iliad. *East West* **1962**, *13*, 317–335.
45. Youso, K. *Afghanistan: Hidden Treasures from the National Museum, Kabul*; Asian Art Museum: San Francisco, CA, USA, 2008.
46. Max, Y. The Enameled Cups from Masada. *J. Glass Stud.* **2021**, *63*, 11–32.
47. Bayley, J. Roman Enamels and Enamelling. In *Glass of the Roman World*; Bayley, J., Freestone, I.C., Jackson, C.P., Eds.; Oxbow Books Ltd.: Oxford, UK, 2015; pp. 178–189.
48. Biek, L.; Butcher, S.A.; Carruthers, T.G.; Rooksby, H.P.; Warren, S.E.; Crummett, J.G.; Hedges, R.E.M.; Kaczmarczyk, A. Enamels and glass pastes on Roman-period 'bronzes' found at Nornour, Isles of Scilly. In *Proceedings of the 16th International Symposium on Archaeometry and Archaeological Prospection*; Slater, E.A., Tate, J.O., Eds.; National Museum of Antiquities of Scotland: Edinburgh, Scotland, 1980; pp. 51–79.
49. Colombari, P. The Destructive/Non-Destructive Identification of Enameled Pottery, Glass Artifacts and Associated Pigments—A Brief Overview. *Arts* **2013**, *2*, 77–110.
50. Caggiani, M.C.; Colombari, P.; Valotteau, C.; Mangone, A.; Cambon, P. Mobile Raman spectroscopy analysis of ancient enamelled glass masterpieces. *Anal. Methods* **2013**, *5*, 4345.
51. Greiff, S.; Schuster, J. Technological study of enamelling on Roman glass: The nature of opacifying, decolourizing and fining agents used with the glass beakers of Lübsow (Lubieszewo, Poland). *J. Cult. Herit.* **2008**, *9*, 27–32.
52. Dussubieux, L.; Gratuze, B. Non-Destructive Characterization of Glass Beads: An application to the study of glass trade between India and Southeast Asia. In Proceedings of the 9th International Conference of the European Association of Southeast Asian Archaeologists, Sigtuna, Stockholm, Sweden, 27 May–2 June 2002; pp. 135–148.

53. Glascock, M.D. Application of Neutron Activation Analysis to Archaeological Studies of Natural and Man-Made Glasses. In *Modern Methods of Analysing Archaeological and Historical Glass, I*; Janssens, K.A., Ed.; John Wiley & Sons, Ltd.: Chichester, UK, 2013; pp. 185–197.
54. Shackley, M. X-Ray Fluorescence (XRF) Analysis in Archaeology. In *X-Ray Fluorescence Spectrometry (XRF) in Geoarchaeology*; Shackley, M., Ed.; Springer: New York, NY, USA, 2011; pp. 7–44.
55. Baert, K.; Meulebroeck, W.; Wouters, H.; Ceglia, A.; Nys, K.; Thienpont, H.; Terryn, H. Raman spectroscopy as a rapid screening method for ancient plain window glass. *J. Raman Spectrosc.* **2011**, *42*, 1055–1061.
56. Weber, G.; Strivay, D.; Martinot, L.; Gamir, H. Use of PIXE-PIGE Under Variable Incident Angle for Ancient Glass Corrosion Measurements. *Nucl. Instrum. Methods Phys. Res. Sect. B Beam Interact. Mater. At.* **2002**, *189*, 350–357.
57. Šmit, Ž. Ion-Beam Analysis Methods. In *Modern Methods of Analysing Archaeological and Historical Glass, I*; Janssens, K.A., Ed.; John Wiley & Sons, Ltd.: Chichester, UK, 2013; pp. 155–184.
58. Fiorentino, S.; Chinni, T.; Vandini, M. Materials Inspiring Methodology: Reflecting the Potential of Transdisciplinary Approaches to the Study of Archaeological Glass. *Appl. Sci.* **2021**, *11*, 8049.
59. Janssens, K. Electron Microscopy. In *Modern Methods of Analysing Archaeological and Historical Glass, I*; Janssens, K.A., Ed.; John Wiley & Sons, Ltd.: Chichester, UK, 2013; pp. 129–154.
60. Campbell, L.; Smith, M. Multi-technique analysis of pigments on sandstone sculptures: Renaissance re-painting of a Roman relief. *Herit. Sci.* **2022**, *10*, 156. <https://doi.org/10.1186/s40494-022-00790-7>.
61. Dyer, J.; Sotiropoulou, S. A technical step forward in the integration of visible-induced luminescence imaging methods for the study of ancient polychromy. *Herit. Sci.* **2017**, *5*, 24.
62. Bracci, S.; Vettori, S.; Cantisani, E.; Degnano, I.; Galli, M. The ancient use of colouring on the marble statues of Hierapolis of Phrygia (Turkey): An integrated multi-analytical approach. *Archaeol. Anthropol. Sci.* **2019**, *11*, 1611–1619.
63. Christie, H.R. *Pushing Boundaries: Spectral Imaging of Archaeological Small Finds*; PhD Thesis, University of Glasgow: Glasgow, Scotland, 2019, Unpublished.
64. Oujja, M.; Sanz, M.; Agua, F.; Conde, J.F.; Garcia-Heras, M.; Dávila, A.; Oñate, P.; Sanguino, J.; Vázquez de Aldana, J.R.; Moreno, P.; et al. Multianalytical characterization of Late Roman glasses including nanosecond and femtosecond laser induced breakdown spectroscopy. *J. Anal. At. Spectrom.* **2015**, *30*, 1590.
65. Donais, M.K.; Van Pevenage, J.; Sparks, A.; Redente, M.; George, D.B.; Moens, L.; Vincze, L.; Vandennebeele, P. Characterization of Roman glass tesserae from Coriglia excavation site (Italy) via energy-dispersive X-Ray fluorescence spectrometry and Raman spectroscopy. *Appl. Phys. A* **2016**, *122*, 1050.
66. Colomban, P.; Kirmizi, B.; Gougeon, C.; Gironde, M.; Cardinal, C. Pigments and glassy matrix of the 17th–18th Century enamelled French watches: A non-invasive on-site Raman and pXRF study. *J. Cult. Herit.* **2020**, *44*, 1–14. <https://doi.org/10.1016/j.culher.2020.02.001>.
67. Collins, R.; Birley, B.; Croom, A.; Laskey, J.; McIntosh, F.; Padley, T.; Parking, A.; Price, E. *Living on the Edge of Empire: The Objects and People of Hadrian's Wall*; Pen and Sword Books Limited: Barnsley, UK, 2020.
68. Birley, B. (Vindolanda Trust, Hexham, UK) Personal communication, 2023.
69. Isings, C. *Roman Glass from Dated Finds*; J.B. Wolters: Groningen, The Netherlands 1957.
70. ©Carole Raddato (CC BY-SA). Available at https://www.flickr.com/search/?user_id=41523983%40N08&sort=date-taken-desc&text=glass%20gladiator&view_all=1 (accessed on 3 April 2023).
71. Hertzberg, G.F. *A History of All Nations from the Earliest Times; Being a Universal Historical Library, Volume 5: Imperial Rome*; Wright, J.H., Translator; Lea Brothers and Company: New York, NY, USA, 1905.
72. Moioli, P.; Seccaroni, C. Analysis of Art Objects Using Portable X-Ray Fluorescence Spectrometer. *X-Ray Spectrom.* **2000**, *29*, 48–52.
73. Fermo, P.; Andreoli, M.; Bonizzoni, L.; Fantauzzi, M.; Guibertoni, G.; Ludwig, N.; Rossi, A. Characterisation of Roman and Byzantine glasses from the surroundings of Thugga (Tunisia): Raw materials and colours. *Microchem. J.* **2016**, *129*, 5–15.
74. Blair, E.H. pXRF Analysis of Heritage Glass. In *Advances in Portable X-Ray Fluorescence Spectrometry: Instrumentation, Application and Interpretation*; Drake, B.L., MacDonald, B.I., Eds.; Royal Society of Chemistry: London, UK, 2022; pp. 400–423.
75. Goldman, Y.; Linn, R.; Shamir, O.; Weinstein-Evron, M. Micro-RTI as a novel technology for the investigation and documentation of archaeological textiles. *J. Archaeol. Sci. Rep.* **2018**, *19*, 1–10. <https://doi.org/10.1016/j.jasrep.2018.02.013>.
76. McConaughy, M.A.; Anderson, G.E.; Harding, D.G. A microscopic examination of materials adhering to two early woodland copper objects from West Virginia and Pennsylvania. *Archaeol. East. N. Am.* **2014**, *42*, 15–24.
77. Jordan, J.M.; Peuramaki-Brown, M.M.; Chiac, S.; Saqui, A.; Tzib, F. It's what's inside that counts: Developing a paste group typology in Belize. *J. Archaeol. Sci. Rep.* **2021**, *37*, 103019. <https://doi.org/10.1016/j.jasrep.2021.103019>.
78. Bustos-Pérez, G.; Díaz, S.; Baena, J. An experimental approach to degrees of rounding among lithic artefacts. *J. Archaeol. Method Theory* **2019**, *26*, 1243–1275. <https://doi.org/10.1007/s10816-018-9409-8>.
79. Kononenko, N.; Torrence, R.; Barton, H.; Hennell, A. Cross-cultural interaction on Wuvulu Island, Papua New Guinea: The perspective from use-wear and residue analysis of turtle bone artifacts. *J. Archaeol. Sci.* **2010**, *37*, 2911–2919. <https://doi.org/10.1016/j.jas.2010.07.001>.
80. Antinozzi, S.; Ronchi, D.; Fiorillo, F.; Barba, S. 3Dino: Configuration for a Micro-Photogrammetric Survey. *Digit. Herit.* **2021**, *2*, 211–222.

81. Tantrakarn, K.; Kato, N.; Nakai, I. The Application of a Portable X-Ray Fluorescence Spectrometer to the On-Site Analysis of Glass Vessel Fragments from Southern Thailand. *Archaeometry* **2012**, *55*, 508–527.
82. Freestone, I.C.; Bimson, M. The Possible Early Use of Chromium as a Glass Colorant. *J. Glass Stud.* **2003**, *45*, 183–185.
83. Colomban, P.; Tournié, A.; Caggiani, M.C.; Paris, C. Pigments and enamelling/gilding technology of Mamluk mosque lamps and bottle. *J. Raman Spectrosc.* **2012**, *43*, 1975–1984.
84. Colomban, P. Polymerization degree and Raman identification of ancient glasses used for jewelry, ceramic enamels and mosaics. *J. Non Cryst. Solids* **2003**, *323*, 180–187.
85. Galli, A.; Bonizzoni, L. True versus forged in the cultural heritage materials: The role of pXRF analysis. *X-Ray Spectrom.* **2014**, *43*, 22–28.
86. Feller, R.L. *‘Artists’ Pigments: A Handbook of Their History and Characteristics*; Cambridge University Press: Cambridge, UK, 1986.
87. Bedford, C.; Robinson, D.W.; Gandy, D. Emigdiano Blues: The California indigenous pigment palette and an in situ analysis of an exotic colour. *Open Archaeol.* **2018**, *4*, 152–172.
88. Ağtürk, T.S. *The Painted Tetrarchic Reliefs of Nicomedia: Uncovering the Colourful Life of Diocletian’s Forgotten Capital*; Brepols: Turnhout, Belgium, 2021.
89. Constantinescu, B.; Cristea-Stan, D.; Szökefalvi-Nagy, Z.; Kovács, I.; Harsány, I.; Kasztovszky, Z. PIXE and PGAA—Complementary methods for studies on ancient glass artefacts (from Byzantine, late medieval to modern Murano glass). *Nucl. Instrum. Methods Phys. Res.* **2018**, *B 417*, 105–109.
90. Amadori, M.L.; Constantini, I.; Madariaga Mota, J.M.; Valentini, L.; Ferrucci, F.; Mengacci, V.; Camaiti, M. Calcium antimonate: A new discovery in colour palette of Paestum wall paintings. *Microchem. J.* **2021**, *168*, 106401.
91. Rütli, B. *Les verres Peints du Haut Empire Romain: Centres de Production et de Diffusion*; Musée Romain: Lausanne, Switzerland, 2001.
92. Whitehouse, D. A Fragment of Roman Glass Decorated with Enamel. *J. Glass Stud.* **2008**, *50*, 306–309.
93. Hassan, I. Transmission electron microscopy and differential thermal studies of lazurite polymorphs. *Am Miner.* **2000**, *85*, 1383–1389.

Disclaimer/Publisher’s Note: The statements, opinions and data contained in all publications are solely those of the individual author(s) and contributor(s) and not of MDPI and/or the editor(s). MDPI and/or the editor(s) disclaim responsibility for any injury to people or property resulting from any ideas, methods, instructions or products referred to in the content.